

Influence of initial soil moisture in a Regional Climate Model study over West Africa. Part 1: Impact on the climate mean

Brahima KONÉ¹, Arona DIEDHIOU^{1, 2}, Adama Diawara¹, Sandrine Anquetin², N'datchoh Evelyne Touré¹, Adama Bamba¹, and Arsene Toka Koba¹

¹LASMES - African Centre of Excellence on Climate Change, Biodiversity and Sustainable Agriculture (ACE CCBAD) / Université Félix Houphouët Boigny, Abidjan, Côte d'Ivoire

²Univ. Grenoble Alpes, IRD, CNRS, Grenoble INP, IGE, F-38000 Grenoble, France

Correspondence to: Arona DIEDHIOU (arona.diedhiou@ird.fr)

Abstract.

The impact of soil moisture initial conditions on the mean climate over West Africa was examined using the latest version of the Regional Climate Model of the International Centre for Theoretical Physics (RegCM4) at a horizontal resolution of 25 km × 25 km. The soil moisture reanalysis of the European Centre Meteorological Weather Forecast's reanalysis of the 20th century ERA20C is used to initialize the control experiment, while its minimum and maximum values over the entire domain are used to establish the initial dry and wet soil moisture conditions respectively (hereafter dry and wet experiments). For the control, the wet and dry experiments, an ensemble of five runs from June to September are performed. In each experiment, we analyzed the two idealized simulations most sensitive to the dry and wet soil moisture initial conditions. The impact of soil moisture initial conditions on precipitation in West Africa is linear over the Central and West Sahel where dry (wet) experiments lead to rainfall decrease (increase). The strongest precipitation increase is found over the West Sahel for wet experiments with a maximum change value of approximately 40%, while the strongest precipitation decrease is found for dry experiments over Central Sahel with a peak of change of approximately -4%. The sensitivity of soil moisture initial condition can persist for three to four months (90-120 days) depending on the region. However, the influence on precipitation is no longer than one month (between 15 and 30 days). The strongest temperature decrease is located over the Central and West Sahel with a maximum change of approximately -1.5 °C in wet experiments, while the strongest temperature increase is found over the Guinea Coast and Central Sahel for the dry experiments, with a maximum of change around 0.6°C. A significant

33 impact of soil moisture initial conditions on the surface energy fluxes is noted: in the wet (dry)
34 experiments, a cooling (warming) of surface temperature is associated with a decrease (increase)
35 of sensible heat flux, an increase (decrease) of latent heat flux and a decrease (increase) of the
36 boundary layer depth. Part II of this study investigates the influence of soil moisture initial
37 conditions on climate extremes.

38 **1 Introduction**

39 In the climate system, soil moisture is a crucial variable that influences water balance and
40 surface energy components through latent surface fluxes and evaporation. Therefore, soil
41 moisture impacts the development of weather patterns and precipitation. The strength of soil
42 moisture impacts on land-atmosphere coupling varies with location and season. Koster et al.
43 (2004) sustained that improving the simulation of the atmospheric response to the slow
44 variations of land and ocean surface conditions may be important for seasonal climate prediction.
45 The atmospheric response to ocean temperature anomalies has been well documented (Diedhiou
46 and Mahfouf 1996; Kirtman et al. 1998; Rasmusson et al.1982). Schär et al. 1999 sustained that
47 the role of soils may be comparable to that of the oceans. The solar energy received by the
48 oceans is stored in summer and used to heat the atmosphere in winter. Conversely, the
49 precipitation received by the soil is stored in winter and the moistening (cooling) is returned to
50 the atmosphere in summer. Through its impact on surface energy fluxes and evaporation, there
51 are many additional impacts on the climate process of soil moisture, such as boundary-layer
52 stability and air temperature (Hong and Pan, 2000; Kim and Hong 2006). Several studies have
53 shown that the anomalies of soil moisture may persist for several weeks or months, however, its
54 impact remains only for a shorter time in the atmosphere, not exceeding few days (Vinnikov and
55 Yeserkepova 1991; Liu et al., 2014). The important role of anomalies in soil moisture in the
56 coupling between land and atmosphere has been shown in several studies, using numerical
57 climate models (Zhang et al., 2011) and observation datasets (Zhang et al., 2008a; Dirmeyer et
58 al., 2006). For instance, over East Asia, Zhang et al., (2011) showed that soil moisture is found
59 to have a much stronger impact on daily maximum temperature variability than on daily mean
60 temperature variability, but generally has small effects on daily minimum temperature, except in
61 the eastern Tibetan Plateau. They showed that soil moisture has a prominent contribution to
62 precipitation variability in many parts of western China.

63
64 West Africa is known to exhibit strong coupling between soil moisture and precipitation (Koster
65 et al., 2004). Several previous studies have been conducted over West Africa on a global scale

66 using atmospheric general circulation model (AGCMs) to investigate the impact of soil moisture
67 initial conditions on the land-atmosphere coupling (Koster et al., 2004; Douville and al, 2001;
68 Zhang et al., 2008b). However, at local and regional scales, the land-atmosphere coupling studies
69 with AGCMs, present significant uncertainties (Xue et al. 2010). The regional climate models
70 (RCMs) have been used to simulate the impact on interannual climate variability of anomalies in
71 soil moisture (Seneviratne et al. 2006; Zhang et al. 2011). These studies have received a lot of
72 attention due to the increase of climate variability associated with extreme weather events that
73 have greater societal and environmental impacts. In general, these studies have been conducted
74 in Asia, Europe and America (e.g. Seneviratne et al. 2006 for Europe; Zhang et al. 2011 for Asia;
75 Zhang et al. 2008b for America). Overall, the results of these studies showed that during
76 summer, the strong impact of the anomalies of soil moisture in land-atmosphere occurred mainly
77 over the transition zones with a climate between wet and dry regimes, in agreement with Koster
78 et al. (2004). The relevance and extent of this potential feedback are still poorly understood in
79 West Africa.

80 This study will focus on the influence of soil moisture initial conditions on climate mean. It is
81 based on performance assessment of the Regional Climate model version 4 coupled to the
82 version 4.5 of the Community Land Model (RegCM4-CLM4.5) performed by Koné et al. (2018)
83 where the ability of the model to reproduce the climate mean has been validated. The
84 descriptions of the model and experimental setup used in this study are presented in Section. 2;
85 in the Section 3, the influence of wet and dry soil moisture initial conditions on the subsequent
86 climate mean is analyzed and discussed; and in Section 4 the main conclusions are presented.
87 While this Part I investigates the impacts on the climate mean, the Part II of this article will be
88 focused on the influence of soil moisture initial conditions on climate extremes.

89 **2. Model and experimental design**

90 **2.1 Model description and observed datasets**

91 The fourth generation of the Regional Climate Model (RegCM4) of the International Centre for
92 Theoretical Physics (ICTP) is used in this study. Since its release, its physical representations
93 have been continuously developed and implemented. The version used in the present study is
94 RegCM4.7. The MM5 (Grell et al., 1994) non-hydrostatic dynamical core has been ported to
95 RegCM without removing the existing hydrostatic core. The model dynamical core used in this
96 study is non-hydrostatic. RegCM4 is a limited area model using a sigma pressure vertical grid
97 and the finite differencing algorithm of Arakawa B-grid (Giorgi et al., 2012). The radiation
98 scheme used in this version of RegCM4.7 is derived from the National Center for Atmospheric

99 Research (NCAR) Community Climate Model Version three (CCM3) (Kiehl et al., 1996).
100 Aerosols representation is from Zakey et al. (2006) and Solomon et al. (2006). The large-scale
101 precipitation scheme is from Pal et al. (2000) and the moisture scheme is the SUBgrid EXplicit
102 moisture scheme (SUBEX). The SUBEX take into account the sub-grid scale cloud variability,
103 and the accretion processes and evaporation for stable precipitation following the work of
104 Sundqvist et al., 1989. In the planetary boundary layer (PBL), the sensible heat over ocean and
105 land, water vapour and turbulent transport of momentum are calculated according to the
106 scheme of Holtslag et al. (1990). Heat and moisture, the momentum fluxes of ocean surfaces in
107 this study are computed as in Zeng et al. (1998). In RegCM4.7, convective precipitation and
108 land surface processes can be described by several parameterizations. Based on Koné et al.
109 (2018), we selected the convective scheme reported by Emanuel (1991) and the interaction
110 processes between soil, vegetation and atmosphere are parameterized with CLM4.5. In each
111 grid cell, CLM4.5 has 16 different Plant Functional Types (PFTs) and 10 soil layers (Lawrence
112 et al., 2011; Wang et al., 2016). RegCM4 is integrated over the domain of West Africa depicted
113 in Fig. 1 with 25 km (182x114 grid points; from 20° W-20° E and 5° S-21° N) with horizontal
114 resolution and with 18 vertical levels and the initial and boundary conditions are taken from the
115 European Centre for Medium-Range Weather Forecasts reanalysis (EIN75; Uppala et al., 2008;
116 Simmons et al., 2007). The sea surface temperatures are obtained from the National Oceanic
117 and Atmosphere Administration (NOAA) optimal interpolation weekly (OI_WK) (Reynolds et
118 al., 1996). The topography data are taken from the States Geological Survey (USGS) Global
119 Multi-resolution Terrain Elevation Data (GMTED; Danielson et al., 2011) at 30 arc-second
120 spatial resolution, which is an update to the Global Land Cover Characterization (GTOPO;
121 Loveland et al., 2000) dataset.

122 Our analysis focuses on precipitation and the 2 m air temperature over the West African domain
123 during the June-July-August-September (JJAS). We validate the simulated precipitation with the
124 dataset from the Climate Hazards Group Infrared Precipitation with Stations (CHIRPS)
125 developed at the University of California at Santa Barbara at the 0.05° high-resolution available
126 from 1981 to 2020 (Funk et al., 2015). The validation of the simulated 2 m temperature relies on
127 the CRU datasets (Climate Research Unit version 3.20) from the University of East Anglia,
128 gridded at a horizontal resolution of 0.5° for 1901 to 2011 (Harris et al., 2013). To facilitate
129 comparison between RegCM4 simulations, all products has been re-gridded to 0.22° × 0.22°
130 using a bilinear interpolation method (Nikulin et al., 2012).

131 **2.2 Experiments setup and analysis methodology**

132 The European 20th Century Weather Prediction Center ERA20C soil moisture reanalysis is used
133 to initialize the control experiment, while its domain-wide minimum and maximum values are
134 used to establish the initial dry and wet soil moisture conditions respectively (hereafter dry and
135 wet experiments). We initialized the dry and wet soil moisture initial conditions (in volumetric
136 fraction $\text{m}^3.\text{m}^{-3}$) respectively at the minimum value ($=0.117*10^{-4}$) and the maximum value
137 ($=0.489$).

138 We designed three experiments (reference, wet, and dry), each with an ensemble of five (5)
139 simulations. The simulation time period for each experiment lasts for 4 months, starting from
140 June 1st to September 30th. The difference between these three experiments is the change in the
141 initial soil moisture condition (reference initial soil moisture condition, wet initial soil moisture
142 condition, and dry initial soil moisture condition) during the first day of the simulation (June 1 st
143 2001, 2002, 2003, 2004 and 2005) over the West African domain. Then, we selected the two
144 runs most impacted by the wet and dry soil moisture initial conditions in order to exhibit the
145 effects on the climate mean beyond the limits of the impacts of RegCM4 initial soil moisture
146 internal forcing. In the same context, several previous studies have selected two extreme years to
147 investigate the climate models sensitivity to soil moisture initial conditions (Hong et al., 2000;
148 Kim and Hong, 2006) outside Africa.

149 Hong and al. (2000) used only two years (three months per year) to investigate the impact of
150 initial soil moisture over North America (in the Great Plains) during two summers spanning
151 May-June-July (MJJ) in 1988 (corresponding to a drought) and 1993 (corresponding to a
152 flooding event). Kim and Hong (2006) selected two contrasting years 1997 (below normal
153 precipitation) and 1998 (above normal precipitation year) for their study over east Asia. The first
154 seven days (Kang et al., 2014) are excluded from the analysis as a spin-up period. Except the
155 geographical location, the experimental setup is the same as that of Hong and Pan (2000). The
156 geographical location of this study is the same as in Koné et al. (2018), with four sub-regions
157 (Fig. 1) exhibiting different features of the annual precipitation cycle: Central Sahel ($10^\circ \text{W} - 10^\circ$
158 $\text{E}; 10^\circ \text{N} - 16^\circ \text{N}$), West Sahel ($18^\circ \text{W} - 10^\circ \text{W}, 10^\circ \text{N} - 16^\circ \text{N}$), and Guinea Coast ($15^\circ \text{W} - 10^\circ$
159 $\text{E}; 3^\circ \text{N} - 10^\circ \text{N}$).

160 In several previous studies (Liu et al., 2014; Hong and Pan, 2000; Kim and Hong, 2006), the
161 mean biases (MB) averaged over their studied domains are used to quantify the impact of the soil
162 moisture initial conditions. In our study, we used the MB and the probability density function
163 (PDF; Gao et al., 2016; Jaeger and Seneviratne, 2011) by fitting a normal distribution to better
164 capture how many grid points are impacted by soil moisture initial conditions. The pattern
165 correlation coefficient (PCC) is also used as a spatial correlation to reveal the degree of large-

166 scale similarity between model simulations and observations. These performance metrics (MB,
167 PCC, and PDF) are computed for both modeled and observed temperature and precipitation only
168 over land grid points.

169 For the two years most sensitive to soil moisture initial conditions, the Student t-test is used to
170 compare the significance of the difference between a wet or dry sensitivity test (sample 1) and
171 the control (sample 2) in assuming that our two samples are independent and in considering that
172 this method performs well for climate simulations compared to more sophisticated techniques
173 developed to address autocorrelation (Damien et al., 2014). The Student t-test is extensively used
174 for analysis in climate sciences; it is fairly robust and easy to use and interpret (Menedez et al.,
175 2019; Talahashi and Polcher, 2019). The Student t-test takes into account, the difference between
176 the means of each sample, the variance (S) and the number of degrees of freedom ($n - 1$), which
177 depends on the sample size (n). The test statistic is calculated as:

$$179 \quad t = \frac{\bar{X}_1 - \bar{X}_2}{\sqrt{\frac{S_1^2}{n_1} + \frac{S_2^2}{n_2}}}$$

178
180 Where \bar{X}_1 (\bar{X}_2) are the sample means, n_1 (n_2) are the sample sizes and S_1^2 (S_2^2) are the sample
181 variances. In this study, the t-test at the 95% confidence level is used to consider statistically
182 significant.

183

184 **3. Results and discussion**

185 **3.1. Influence of soil moisture initial conditions on precipitation.**

186 To identify the two runs most impacted by the dry and wet experiments among the ensemble of
187 five simulations (initiated on 1st June 2001, 2002, 2003, 2004 and 2005), we superimposed on
188 Figure 2, the magnitude of daily soil moisture changes of the 5 runs compared to their
189 corresponding control experiment over West African domain. Figure 2 shows that for the dry
190 experiments (negative values of daily soil moisture changes), the weakest and strongest impacts
191 of soil moisture initial conditions are found with the runs initiated on 1st June 2004 and 2003
192 respectively. For the wet experiments (positive values of daily soil moisture changes), the
193 weakest impact is found for the run initiated on 1st June 2003, while the other runs exhibit quite
194 the same strong sensitivity. From these results, we selected the two runs initiated on June 1st,
195 2003 and June 1st, 2004 as the simulations most influenced by the initial wet and dry soil
196 moisture conditions, respectively, to better highlight the effects on the climate mean beyond the

197 limits of the impact of the initial internal soil moisture forcing. It is worth noting that 2003 is
198 wetter than 2004 and is more sensitive to the dry experiment. While 2004 which is drier than
199 2003 is more sensitive to the wet experiment.

200
201 Figure 3 displays the spatial distribution of the observed mean rainfall (mm/day) from CHIRPS
202 (Fig. 3a, c) for the runs JJAS 2003 and JJAS 2004 and the simulated from control experiments
203 (Fig. 3b, d) initialized with reanalysis soil moisture ERA20C. Table 1 reports the MB and PCC
204 for model simulation compared to CHIRPS, computed for the Central Sahel, Guinea Coast, West
205 Sahel, and the entire West African domain. The CHIRPS product displays a zonal band of
206 rainfall centered around 10° N, decreasing from North to South (Fig. 3a, c). The maximum
207 values are located over the mountain regions of Cameroun and Guinea. While the precipitation
208 minimum values are found over the Sahel and the Sahara. The control experiments (Fig. 3 b and
209 d) reproduced the large-scale pattern of observed rainfall with PCC = 0.72 and 0.77 for the runs
210 JJAS 2003 and JJAS 2004, respectively (Table 1). The spatial extent of rainfall maxima and the
211 North-South gradient are well captured by control experiments; however, their magnitudes are
212 underestimated with respect to the CHIRPS observation. Over West African domain, dry MB
213 reaching -49.31% and -50.56% are obtained for the runs JJAS 2003 and JJAS 2004,
214 respectively (Table 1). Fig. 4 displays the change in mean precipitation (in %) in JJAS 2003 and
215 JJAS 2004 for dry and wet experiments with respect to the control experiments. The dotted area
216 shows changes with a statistical significance of 95%.

217
218 Dry and wet sensitivity experiments showed that precipitation is significantly affected by soil
219 moisture initial conditions at magnitude varying with the sub-regions (Fig. 4). Over the Central
220 Sahel, for the dry experiments (Fig. 4a, c), we found a precipitation decrease for JJAS 2003 and
221 JJAS 2004 (Fig. 4a, c). On the other hand, over the Guinea coast, we found an increase in rainfall
222 for both JJAS 2003 and JJAS 2004. For the wet experiments (Fig.4b, d), there is an increase of
223 rainfall over most of studied domains for both JJAS 2003 and JJAS 2004. Overall, the impact of
224 the soil moisture initial conditions on the precipitation is linear only over the Central Sahel for
225 both JJAS 2003 and 2004. Therefore, the dry (wet) experiments exhibits significant decrease
226 (increase) in precipitations with respect to the control experiments (Fig.4a, c).

227
228 For a better quantitative evaluation, the PDF distributions of precipitation changes in JJAS 2003
229 and JJAS 2004, over (a) central Sahel, (b) west Sahel, (c) Guinea coast and (d) West Africa
230 obtained from dry and wet experiments with respect to the control experiments are shown in Fig.

231 5. Table 2 summarizes the maximum values of changes obtained from the PDF's of the different
232 variables used in this study. The impact on precipitation of the soil moisture initial conditions is
233 linear only over Central Sahel (Fig.5a) where the change in dry (wet) experiments showed a
234 precipitation decrease (increase). The strongest precipitation increase is found over West Sahel
235 for the wet **experiment** with maximum change reached 40%. However, the strongest
236 precipitation decrease is found over the Central Sahel for dry experiment with a maximum
237 change value about -4% (Table 2). We noted that the impacts on precipitation of the wet
238 experiments are greater than those from dry experiments (Table 2). These results are consistent
239 with previous studies that supported a strong relationship between precipitation and soil moisture
240 in particular over the transition zones with a climate between wet and dry climate regimes
241 (Koster et al., 2004; Liu et al., 2014; Douville et al., 2001).

242
243 Fig. 6 and Fig. 7 shows the changes in the daily soil moisture and precipitation, respectively,
244 from dry and wet experiments with respect to the control experiments, during the runs JJAS
245 2003 and JJAS 2004. To compute the changes of daily soil moisture, we considered the second
246 top soil layer in CLM4.5 (from 0 to 2.80 cm). In general, the impacts of soil moisture initial
247 conditions on the daily soil moisture persist from three to four months over the studied domains
248 (Fig.6). The strongest duration and amplitude of the impact on the daily soil moisture is found
249 over the West Sahel sub-region. The impact on the daily soil moisture lasts four months in JJAS
250 2003 and JJAS 2004. For wet experiments, the weakest duration of the impact of soil moisture
251 initial conditions is found over the Guinea Coast and lasts three months (Fig. 6c). While, for dry
252 experiments, the weakest impact on the daily soil moisture is found over Central Sahel and lasted
253 three months (Fig. 6a). These results are in line with previous works which argued that the soil
254 moisture-atmosphere feedback strength and the land memory are place dependent (Vinnikov et
255 al. 1996; Vinnikov and Yeserkepova 1991).

256 Figure 7 shows the changes of the daily precipitation to the soil moisture initial conditions over
257 the different studied domains. The impact of the wet experiments on daily precipitation is greater
258 in magnitude than that of dry experiments over most studied domains (Fig. 7). For dry
259 experiments, the strongest daily precipitation response (about $-4\text{mm}\cdot\text{day}^{-1}$), is found over the
260 Guinea Coast in the run JJAS 2003 (Fig. 7c). While for the wet experiments, the strongest impact
261 on the daily precipitation is more than $8\text{mm}\cdot\text{day}^{-1}$ and it is found over the West Sahel and the
262 Guinea Coast (Fig. 7b, c, respectively). It is worth to note that the impact of initial soil moisture
263 conditions on daily precipitation is much shorter than the duration of the impact on daily soil
264 moisture. The significant impact on daily precipitation is found only for wet experiments, and

265 did not last more than 15 days in large parts of the study domain, excepted over wetter sub-
266 region of Guinea Coast where it lasts approximately one month. We noted that the precipitation
267 peaks over West Sahel and Guinea Coast (Fig. 7b and c, respectively) during August and
268 September coincide with fluctuation in the daily soil moisture impact (Fig.6b and c). This
269 probably indicates the strong feedback of soil moisture and precipitation during this period over
270 the Guinea Coast and West Sahel regions.

271 To investigate the causes of the precipitation changes, we examined the vertical profile change in
272 relative humidity and air temperature for the runs JJAS 2003 and JJAS 2004, respectively, from
273 dry and wet experiments with respect their control experiment.

274 The impacts on relative humidity and air temperature (Fig.8 and Fig.9, respectively) of soil
275 moisture initial conditions are significant in the lower troposphere. In the low and mid-
276 troposphere, a drying and a warming are found in the dry experiments, while a moistening and a
277 cooling are simulated in the wet experiments. This indicates that a weak (strong) dry convection
278 is found over most of the studied domains for dry (wet) experiments. The strongest impact on the
279 relative humidity and temperature in the lower and middle troposphere is found over central
280 Sahel (Fig.8a and Fig. 9a).

281 For the upper troposphere, the significant impact on relative humidity and temperature is found
282 only for wet experiments, and exhibited a drying and a warming over most of studied domains
283 (Fig.8 and Fig.9). This impact for the wet experiments was also reported by Hong and Pal
284 (2000).

285 To understand other causes of the precipitation changes illustrated in Fig. 4, we analyzed the
286 changes in lower tropospheric wind (850hpa) and specific humidity for the runs JJAS 2003 and
287 JJAS 2004 during the dry and wet experiments with respect to the control experiments (Fig. 10).

288 For the dry experiments (Fig. 10a, c), we found that the moistening of the lower atmosphere
289 decreases over most of the study domain. However, the strong wind magnitude changes over the
290 Atlantic Ocean bring the moistening from the ocean to the Guinea Coast and West Sahel. This
291 can explain the precipitation increase over these sub-regions in the dry experiments. Over
292 Central Sahel, the strong decrease in precipitation seems to be associated with the decrease of
293 specific humidity which is particularly notable in the run JJAS 2003 (Fig.4a). Conversely, for the
294 wet experiments (Fig.10b, d), an increase in the moistening of the atmosphere is found mainly
295 over the Sahel band while further South, a decrease of the specific humidity is simulated over
296 Guinea Coast. The strong change in wind magnitude shifts the moistening from the North to the
297 South, leading to precipitation increase over most part of study domain (Fig.4 b and d). These

298 results are broadly consistent with precipitation changes for dry and wet experiments shown in
299 Figure 4.

300 Summarizing these results, the impact of soil moisture initial conditions is linear only over the
301 Central Sahel for the runs JJAS 2003 and 2004. The strongest precipitation decrease is found
302 over Central Sahel for the dry experiment in the run JJAS 2003 with maximum change reaching
303 -4% . While, the strongest precipitation increase is found over the West Sahel for the wet
304 experiment in the run JJAS 2004 with maximum change about 40% . The impact of soil moisture
305 initial conditions on daily soil moisture can persist for three to four months according to the sub-
306 domains, while the significant impact on precipitation (greater than $1\text{mm}\cdot\text{day}^{-1}$) is much shorter
307 and no longer than one month. The impact of soil moisture initial conditions is mostly confined
308 at the near-surface climate and somewhat at the upper troposphere.

309 **3.2. Influence on temperature and other surface fluxes.**

310 Figure 11 shows the spatial distribution of the mean observed 2m temperature from CRU during
311 JJAS 2003 and JJAS 2004 (Fig. 11a, c, respectively) and the mean simulated temperature from
312 the control experiments of runs JJAS 2003 and JJAS 2004 (Fig.11 b, d, respectively) initialized
313 with ERA20C. Table 3 summarizes the PCC and MB between model simulations of temperature
314 with respect to CRU, calculated for the West Sahel, Central Sahel, Guinea Coast and the entire
315 West African domain. The CRU temperature displays a zonal distribution over the whole West
316 Africa domain. Maximum values of approximately $34\text{ }^{\circ}\text{C}$ are found over the Sahara, while the
317 lowest temperatures not exceed 26°C , are located over the Guinea Coast especially in orographic
318 regions such as Guinean highlands, Cameroon Mountains and the Jos Plateau. The control
319 experiments (Fig. 11b, d) showed good agreement in the representation of the large-scale pattern
320 of CRU observation, with PCC about 0.99 for both JJAS 2003 and JJAS 2004 (Table 3),
321 including the meridional gradient between Sahara Desert and Guinea Coast which is crucial for
322 the African Easterly Jet evolution and formation (Thorncroft and Blackburn 1999; Cook 1999).
323 The spatial extent of temperature maxima and minima are well reproduced by control
324 experiments, however their magnitudes are overestimated compared to CRU. The strongest
325 warm MB of control experiments relative to CRU are approximately $2.68\text{ }^{\circ}\text{C}$ and $2.14\text{ }^{\circ}\text{C}$
326 respectively for JJAS 2003 and JJAS 2004; they are found over the West Sahel (Table 3).

327 Figure 12 shows changes in mean temperature for the runs JJAS 2003 and JJAS 2004 of dry and
328 wet experiments with respect to the control experiments. The dots show areas where impacts of
329 soil moisture initial condition are statistically significant at the 0.05 level. In the dry experiments,
330 for both JJAS 2003 and JJAS 2004 runs, the warmest changes are located under the latitude 13°

331 N, with maximum values located over the Guinea coast. For the wet experiments, the coolest
332 changes are found over the West and Central Sahel.

333 For a better quantitative evaluation, the PDF distributions of the changes in mean temperature in
334 runs JJAS 2003 and JJAS 2004 are showed in Figure 13. The impact on temperature is linear
335 over the Central Sahel, Guinea Coast and the whole West African domain (Fig.13a, c and d). The
336 strongest mean temperature decrease is observed over the Central and West Sahel in wet
337 experiments with the maximum change approximately $-1.5\text{ }^{\circ}\text{C}$ (Table 2). However, the strongest
338 increase of mean temperature is found over the Central Sahel (JJAS 2003) and the Guinea coast
339 (JJAS 2004) in dry experiments reaching $0.56\text{ }^{\circ}\text{C}$ and 0.59°C , respectively (Table 2). Overall,
340 the impact in the dry (wet) sensitivity experiments on 2m-temperature showed an increase
341 (decrease) in warming (cooling) for both JJAS 2003 and JJAS 2004 over most of the studied
342 domains. The exception is found over the west Sahel, where both dry and wet experiments lead
343 to temperature increase (Fig.13, Table2).

344 We now analyze the influence of soil moisture initial conditions anomalies on land energy
345 balance, particularly on the surface fluxes sensible and latent heat. Figure 14 shows changes in
346 sensible heat fluxes (in $\text{W}\cdot\text{m}^{-2}$) in runs JJAS 2003 and JJAS 2004, from dry and wet experiments
347 compared to the control experiments. The dots show changes that are statistically significant at
348 the 0.05 level. As shown in figure 14, the impact on sensible fluxes of soil moisture initial
349 conditions is strong. It is linear over most of the studied domains: the dry (wet) experiments with
350 respect to the control exhibits significant increase (decrease) of the sensible heat (Fig.14).

351 The PDF distributions of change in sensible heat flux are displayed in Figure 15. The dry (wet)
352 experiments showed an increase (a decrease) of the sensible flux in both runs JJAS 2003 and
353 JJAS 2004 (Fig. 15). The impact in wet experiments is strong over Central and West Sahel
354 compared to the dry experiments, but not for Guinea Coast (Fig. 15, Table 2). In the dry
355 experiments, the strongest sensible heat flux increase is found over Guinea Coast, with
356 maximum change about $9.18\text{ W}\cdot\text{m}^{-2}$ during JJAS 2004 (see Table 2). In the wet experiments, the
357 strongest sensible heat flux decrease is located over Central Sahel with maximum change about
358 $-39.66\text{ W}\cdot\text{m}^{-2}$ during JJAS 2003 (see Table 2).

359
360 Unlike the case of sensible heat flux, changes in latent heat showed a linear opposite patterns.
361 Dry experiments result in latent heat flux decrease, while the wet experiments result in latent
362 heat flux increase over most of studied domains (Fig. 16). The PDF distributions of latent heat
363 flux changes are shown in Figure 17. In the wet experiments, the strongest latent heat flux
364 increase is found over West Sahel with maximum change reaching $36.49\text{ W}\cdot\text{m}^{-2}$ in JJAS 2004

365 (Table2). In the dry experiments, the strongest latent heat flux decrease is located over Guinea
366 Coast with maximum change reaching -14.64 W.m^{-2} in JJAS 2004 (Table2). It is worth to note
367 that the impacts on latent and sensible heat flux in wet experiments are stronger compared to
368 those in the dry experiments over most of studied domains, except over Guinea Coast (Table 2).

369
370 We then examined the impact on the stability of the PBL of the soil moisture initial conditions.
371 Different spatial distributions of surface fluxes significantly affect the boundary layer
372 development. Soil moisture can influence rainfall by limiting evapotranspiration, which affects
373 the development of the daytime PBL and thereby the initiation and intensity of convective
374 precipitation (Eltahir, 1998). Figure 18 shows changes in PBL (in m) for JJAS 2003 and JJAS
375 2004, from dry and wet experiments with respect to the control experiments with dotted areas
376 that are statistically significant at the 0.05 level. The soil moisture initial conditions impact
377 significantly the PBL. The dry experiments show PBL increase under the latitude 15°N for both
378 JJAS 2003 and JJAS 2004 (Fig.18 a and c, respectively). For the wet experiments, a PBL
379 decrease is found over most of the studied domains. The PDF of PBL changes (Fig. 19) show
380 that the impact on PBL is linear over most of studied domains. The dry (wet) experiments lead to
381 an increase (decrease) of PBL for both JJAS 2003 and JJAS 2004. The strongest PBL increase
382 (decrease) is found over Guinea Coast (West Sahel) in dry (wet) experiments during JJAS 2004
383 (JJAS 2003) reaching 146.80m (-293.23m). A dry (wet) air is located above the areas where
384 PBL increase (decrease), causing the air column to become warm (cool) and dry (moist) for the
385 dry (wet) experiment (see Fig. 8 and Fig. 9). These results are consistent with the work of Hong
386 and Pan (2000).

387 Summarizing the results of this section, we found that in the wet experiments, the cooling of the
388 mean temperature is associated with an increase of the latent heat flux, a decrease of the sensible
389 heat flux and of the PBL depth over most studied domain. Conversely, in the dry experiments,
390 the warming of surface temperature is associated with a decrease of latent heat, an increase of
391 sensible heat flux and PBL depth.

392 **4. Conclusion**

393 The impact of the soil moisture initial conditions on the subsequent summer (JJAS) mean
394 climate over West Africa was explored using the RegCM4-CLM45. In particular, the aim of this
395 study was to investigate how soil moisture initialization at the beginning of the rainy season may
396 affect the intra-seasonal variability of temperature and precipitation mean within the subsequent
397 season (June to September).

398 For this purpose, we set up three numerical experiments with RegCM4 in which we applied, at
399 the first day (June 1st), a control soil moisture initial condition (control experiment), a wet soil
400 moisture initial condition (wet experiment), and a dry soil moisture initial condition (dry
401 experiment). For each experiment, an ensemble of five simulations beginning from June 1st to
402 September 30th(JJAS), for the years 2001 to 2005 is performed. In this paper, we present results
403 of the two runs JJAS 2003 and JJAS 2004 most impacted by soil moisture dry and wet initial
404 conditions respectively to avoid effects of initial soil moisture internal forcing.

405 The impact of soil moisture initial conditions on precipitation is linear only over the Central
406 Sahel for both JJAS 2003 and JJAS 2004, and over the West Sahel especially in JJAS 2004. In
407 the dry experiment, the strongest precipitation decrease is found over the Central Sahel in JJAS
408 2003 with maximum change reaching -4% while in the wet experiment, the strongest
409 precipitation increase is found over the West Sahel in JJAS 2004 with maximum change
410 reaching 40% . The impact of soil moisture initial conditions can persist for three to four months
411 (90-120 days) depending on the sub-region but the impact on precipitation is no longer than 30
412 days (15 days over the Sahel and 30 days over the Guinea Sahel). This study shows that when
413 averaged over the entire West African region, the sensitivity of rainfall to initial soil moisture
414 conditions is not captured. However, it is important to have a good initialization of soil moisture
415 because depending on the region, the sensitivity of rainfall can be more or less strong. Indeed,
416 rainfall is more sensitive to initial soil moisture conditions in the western and central Sahel (arid
417 zones) than in the Guinean Coast (humid zone). In these arid Sahelian zones, wetter initial
418 conditions will result in more rainfall, especially in the West Sahel, and dry initial conditions
419 will result in less rainfall, especially in the Central Sahel. In the Guinean Coast, the sensitivity of
420 precipitation to initial soil moisture conditions is lower and other factors could be involved such
421 as moisture advection from the Atlantic by the monsoon flow (Koné et al., 2018) and a lower
422 albedo (Charney 1975).

423 Our results show that soil moisture wet initial conditions lead in the lower troposphere to an
424 increase of relative humidity associated with a cooling of air temperature and in the upper
425 troposphere, to a decrease of relative humidity and a warming of air temperature. While the dry
426 experiments mainly impact the lower troposphere with a decrease of the relative humidity
427 associated with a warming air temperature.

428 The temperature at 2m is more sensitive to the anomalies of initial soil moisture condition than
429 the precipitation. The strongest impact on 2m-temperature is found over the Central Sahel with a
430 maximum change about -1.5 °C and 0.6 °C for the wet and dry experiments, respectively.

431 Our study showed significant impacts of soil moisture initial conditions on the surface energy
432 fluxes. For the wet experiments, we found that the cooling of surface temperature is associated
433 with a decrease of the sensible heat flux, an increase of the latent heat flux and a decrease of the
434 PBL depth. For the dry experiments, the warming of surface temperature is associated with an
435 increase of the sensible heat flux, a decrease of the latent heat flux and an increase of the PBL
436 depth.

437 This study showed that soil moisture as a boundary condition plays a major role in controlling
438 summer climate variability not only over the Sahel band but also over humid zones such as
439 Guinea Coast. Therefore, the good prescription of soil moisture initial conditions could improve
440 the simulation of precipitation and temperature, which would help to reduce biases in climate
441 model simulations. Overall, land surface initialization can contribute to improving sub-seasonal
442 to seasonal forecast skill, but this requires further investigation.

443 This study is the first investigating the impact of soil moisture initial conditions in West Africa.
444 However, this study is based on idealized experiments: sensitivity experiments such as "wet" and
445 "dry" ones conducted in this study were not intended to simulate real climate since such
446 extremes are very rare. Moreover, this study is very specific to RegCM4. In the future, an
447 investigation using different RCMs in a multi-model framework will contribute to better quantify
448 the impact of soil moisture initial conditions. At shorter timescales, there is a need to understand
449 how the soil moisture initial conditions contribute to the triggering and the maintenance of the
450 mesoscale convective systems which are known to explain large amount of rainfall in the region
451 (Mathon et al., 2002). Finally, in the context of climate change, considering the projected
452 increase of high-impact weather events in the region, there is a need to explore the sensitivity of
453 soil moisture initial conditions to climate extremes.

454

455 **Authors contributions**

456 The authors declare to have no conflict of interest with this work. B. Koné and A. Diedhiou fixed
457 the analysis framework. B. Koné carried out all the simulations and figures production according
458 to the work plan proposed by A. Diedhiou. Figures for this manuscript were prepared by B. Koné
459 according the outline proposed by A. Diedhiou and A. Diawara. All authors contributed to the
460 analyses and to the drafting of this manuscript.

461 **Acknowledgements**

462 The research leading to this publication is co-funded by the NERC/DFID "Future Climate for
463 Africa" programme under the AMMA-2050 project, grant number NE/M019969/1 and by IRD

464 (Institut de Recherche pour le Développement; France) grant number UMR IGE Imputation
465 252RA5.

466

467

468

469 **References:**

470

471 Beljaars A. C. M., Viterbo P., Miller M. J., and Betts A. K.: The anomalous rainfall over the
472 United States during July 1993: Sensitivity to land surface parameterization and soil moisture
473 anomalies, *Mon. Weather Rev.*, 124(3), 362–382, doi:10.1175/1520-0493(1996)124<0362:
474 TAROTU>2.0.CO;2, 1996.

475

476 Bosilovich, M. G., and Sun W. Y.: Numerical simulations of the 1993 Midwestern flood: Land–
477 atmosphere interactions. *J. Climate*, 12, 1490–1505, 1999.

478

479 Charney, J. G. Dynamics of deserts and drought in the Sahel. *Quarterly Journal of the Royal*
480 *Meteorological Society*, 101(428), 193-202. <https://doi-org/10.1002/qj.49710142802>, 1975.

481

482 Cook K. H.: Generation of the African easterly jet and its role in determining West African
483 precipitation, *J. Climate*, 12, 1165–1184, [https://doi.org/10.1175/1520-0442\(1999\)012](https://doi.org/10.1175/1520-0442(1999)012)
484 <1165:GOTAEJ> 2.0.CO;2, 1999.

485

486 Damien Decremer, Chul E. Chung, Annica M. L. Ekman & Jenny Brandefelt (2014) Which
487 significance test performs the best in climate simulations?, *Tellus A: Dynamic Meteorology and*
488 *Oceanography*, 66:1, DOI: 10.3402/tellusa.v66.23139.

489

490 Danielson J.J., and Gesch D.B.: Global multi-resolution terrain elevation data 2010
491 (GMTED2010): U.S. Geological Survey Open-File Report 2011–1073, 26 p, 2011.

492

493 Diedhiou, A., & Mahfouf, J. F. Comparative influence of land and sea surfaces on the Sahelian
494 drought: a numerical study. In *Annales Geophysicae* (Vol. 14, No. 1, pp. 115-130). Copernicus
495 GmbH, <https://doi.org/10.1007/s00585-996-0115-6>. 1996.

496
497 Dirmeyer P. A., Koster R. D., and Guo Z.: Do global models properly represent the feedback
498 between land and atmosphere, *J. Hydrometeorol.*, 7(6), 1177–1198, doi:10.1175/JHM532.1,
499 2006.
500
501 Douville, F. Chauvin, and H. Broqua.: Influence of soil moisture on the Asian and African
502 monsoons. Part I: Mean monsoon and daily precipitation. *J. Climate*, 14, 2381–2403, 2001.
503
504 Eltahir E. A. B.: A soil moisture-rainfall feedback mechanism 1. Theory and observations, *Water*
505 *Resour. Res.*, 34, 765–776, doi:10.1029/97WR03499, 1998.
506
507 Emanuel K. A.: A scheme for representing cumulus convection in large-scale models. *Journal of*
508 *the Atmospheric Science* 48: 2313–2335, 1991.
509
510 Funk, C., Peterson, P., Landsfeld, M. et al. The climate hazards infrared precipitation with
511 stations—a new environmental record for monitoring extremes. *Sci Data* 2, 150066 (2015).
512 <https://doi.org/10.1038/sdata.2015.66>
513
514 Gao, X.-J., Shi, Y., and Giorgi, F.: Comparison of convective parameterizations in RegCM4
515 experiments over China with CLM as the land surface model, *Atmos. Ocean. Sci. Lett.*, 9, 246–
516 254, <https://doi.org/10.1080/16742834.2016.1172938>, 2016.
517
518 Giorgi F., Coppola E., Solmon F., Mariotti L., Sylla M. B., Bi X., Elguindi N., Diro G. T., Nair
519 V., Giuliani G., Cozzini S., Guettler I., O’Brien T., Tawfik A., Shalaby A., Zakey A. S., Steiner
520 A., Stordal F., Sloan L., and Brankovic C.: RegCM4: model description and preliminary tests
521 over multiple CORDEX domains, *Clim. Res.*, 52, 7–29, <https://doi.org/10.3354/cr01018>, 2012.
522
523 Grell G., Dudhia J. and Stauffer D. R.: A description of the fifth generation Penn State/NCAR
524 Mesoscale Model (MM5), National Center for Atmospheric Research Tech Note NCAR/TN-
525 398+STR, NCAR, Boulder, CO, 1994.
526
527 Harris I., Jones P. D., Osborn T. J. and Lister D. H.: Updated high-resolution grids of monthly
528 climatic observations, *Int. J. Climatol.*, 34, 623–642, <https://doi.org/10.1002/joc.3711>, 2013.

529
530 Holtslag A., De Bruijn E., and Pan H. L.: A high resolution air mass transformation model for
531 short-range weather forecasting, *Mon. Weather Rev.*, 118, 1561–1575, 1990.
532
533 Hong S-Y. and Pan H-L.: Impact of soil moisture anomalies on seasonal, summertime
534 circulation over North America in a regional climate model. *J. Geophys. Res.*, 105 (D24), 29
535 625–29 634, 2000.
536
537 Jaeger E. B., and Seneviratne S.I.: Impact of soil moisture-atmosphere coupling on European
538 climate extremes and trends in a regional climate model, *Clim. Dyn.*, 36(9-10), 1919-1939,
539 doi:10.1007/s00382-010-0780-8, 2011.
540
541 Kang S, Im E.-S. and Ahn J.-B.: The impact of two land-surface schemes on the characteristics
542 of summer precipitation over East Asia from the RegCM4 simulations *Int. J. Climatol.* 34: 3986-
543 3997, 2014.
544
545 Kiehl J., Hack J., Bonan G., Boville B., Breigleb B., Williamson D., Rasch P.; Description of the
546 NCAR Community Climate Model (CCM3). National Center for Atmospheric Research Tech
547 Note NCAR/TN-420+STR, NCAR, Boulder, CO, 1996.
548
549 Kim J-E., and Hong S-Y.: Impact of Soil Moisture Anomalies on Summer Rainfall over East
550 Asia: A Regional Climate Model Study, *Journal of Climate*. Vol. 20, 5732–5743, DOI:
551 10.1175/2006JCLI1358.1, 2006.
552
553 Kirtman B.P., Schopf P. S.: Decadal Variability in ENSO Predictability and Prediction. *Journal*
554 *of Clim.* 11, 2804, 1998.
555
556 Koné B., Diedhiou A., N’datchoh E. T., Sylla M. B., Giorgi F., Anquetin S., Bamba A., Diawara
557 A., and Koba A. T.: Sensitivity study of the regional climate model RegCM4 to different
558 convective schemes over West Africa. *Earth Syst. Dynam.*, 9, 1261–1278.
559 <https://doi.org/10.5194/esd-9-1261-2018>, 2018.
560
561 Koster R. D., Dirmeyer P. A., Zhichang G., Bonan G., Chan E., Cox P., Gordon C. T., Kanae S.,
562 Kowalczyk E., Lawrence D., Liu P., Lu C. H, Malyshev S., McAvaney B., Mitchell K, Mocko

563 D., Oki T., Oleson K., Pitman A., Sud Y. C., Taylor C. M., Verseghy D., Vasic R., Xue Y.,
564 Yamada T.: Regions of strong coupling between soil moisture and precipitation, *Science*, 305,
565 1138–1140, doi:10.1126/science.1100217, 2004.

566

567 Lawrence D.M., Oleson K.W., Flanner M.G., Thornton P.E., Swenson S.C., Lawrence P.J., Zeng
568 X., Yang Z.-L., Levis S., Sakaguchi K., Bonan G.B., and Slater A.G.:Parameterization
569 improvements and functional and structuraladvances in version 4 of the Community Land
570 Model. *J. Adv. Model. Earth Sys.* 3. DOI:10.1029/2011MS000045, 2011.

571

572 Liu D., WangG. L., Mei R., Yu Z. B. and Gu H. H.: Diagnosing the strength of land-atmosphere
573 coupling at sub-seasonal to seasonal time scales in Asia, *J. Hydrometeor.*, doi:10.1175/JHM-D-
574 13-0104.1, 2013.

575

576 Liu D., G. Wang R. Mei Z. Yu, and Yu M.: Impact of soil moisture initial conditions anomalies
577 on climate mean and extremes over Asia, *J. Geophys. Res. Atmos.*, 119, 529–545,
578 doi:10.1002/2013JD020890, 2014.

579

580 Loveland, T. R., Reed, B. C., Brown, J. F., Ohlen, D. O., Zhu, J., Yang, L., and Merchant, J. W.:
581 Development of a global land cover characteristics database and IGBP DISCover from 1-km
582 AVHRR Data, *Int. J. Remote. Sens.*, 21, 1303–1330, 2000.

583

584 Mathon, V., Diedhiou, A., & Laurent, H. (2002). Relationship between easterly waves and
585 mesoscale convective systems over the Sahel. *Geophysical research letters*, 29(8), 57-1.

586

587 Menéndez, C. G., Giles, J., Ruscica, R., Zaninelli, P., Coronato, T., Falco, M., ... & Li, L. (2019).
588 Temperature variability and soil–atmosphere interaction in South America simulated by two
589 regional climate models. *Climate Dynamics*, 53(5), 2919-2930.

590

591 Oglesby R. J., and Erickson III D. J.: Soil moisture and the persistence of North American
592 drought. *J. Climate*, 2, 1362–1380, 1989.

593

594 Oglesby R. J., Marshall S., Erickson III D. J., Roads J. O. and Robertson F. R.: Thresholds in
595 atmosphere-soil moisture interactions: Results from climate model studies. *J. Geophys. Res.*,107,
596 4244, doi:10.1029/2001JD001045, 2002.

597
598 Oleson K., Lawrence D. M., Bonan G. B., Drewniak B., Huang M., Koven C. D., Yang Z. -L.:
599 Technical description of version 4.5 of the Community Land Model (CLM) (No. NCAR/TN-
600 503+STR). doi:10.5065/D6RR1W7M, 2013.
601
602 Paeth H., Girmes R., Menz G. and Hense A.: Improving seasonal forecasting in the low latitudes,
603 *Mon. Weather Rev.*, 134, 1859-1879, 2006.
604
605 Pal J. S., Small E. E. and Elthair E. A.: Simulation of regional scale water and energy budgets:
606 representation of subgrid cloud and precipitation processes within RegCM, *J. Geophys. Res.*,
607 105, 29579–29594, 2000.
608
609 Pal J. S. and Eltahir E. A. B.: Pathways relating soil moisture conditions to future summer
610 rainfall within a model of the land–atmosphere system. *J. Climate*, 14, 1227–1242, 2001.
611
612 Peterson T. C., Folland C., Gruza G., Hogg W. Mokssit A., Plummer N.: Report on the activities
613 of the working group on climate change detection and related rapporteurs 1998-2001. Geneva
614 (Switzerland): WMO Rep. WCDMP 47, WMO-TD 1071, 2001.
615
616 Nicholson S. E.: The West African Sahel: a review of recent studies on the rainfall regime and its
617 interannual variability, *Meteorology*, 453521, 32 p., <https://doi.org/10.1155/2013/453521>, 2013.
618
619 Nikulin G., Jones C., Samuelsson P., Giorgi F., Asrar G., Büchner M., Cerezo-Mota R.,
620 Christensen O. B., Déque M., Fernandez J., Hansler A., van Meijgaard E., Sylla M. B. and
621 Sushama L.: Precipitation climatology in an ensemble of CORDEX-Africa regional climate
622 simulations, *J. Climate*, 6057–6078, <https://doi.org/10.1175/JCLI-D-11-00375.1>, 2012.
623
624 Rasmusson E. M. and Carpenter T. H.: Variations in Tropical Sea Surface Temperature and
625 Surface Wind Fields Associated with the Southern Oscillation/El Niño. *Mon. Weather Rev.* 110,
626 354, 1982.
627
628 Reynolds, R. W. and Smith, T. M.: Improved global sea surface temperature analysis using
629 optimum interpolation, *J. Climate*, 7, 929–948, 1994.

630 Seager R., and Vecchi G. A.: Greenhouse warming and the 21st century hydroclimate of
631 southwestern North America. *Proc. Natl. Acad. Sci. USA*, 107, 21 277–21 282,
632 doi:10.1073/pnas.0910856107, 2010.

633

634 Simmons A. S., Uppala D. D. and Kobayashi S.: ERA-interim: new ECMWF reanalysis products
635 from 1989 onwards, *ECMWF Newsl.*, 110, 29–35, 2007.

636

637 Solmon F., Giorgi F., and Liousse C.: Aerosol modeling for regional climate studies: application
638 to anthropogenic particles and evaluation over a European/African domain, *Tellus B*, 58, 51–72,
639 2006.

640

641 Sundqvist H. E., Berge E., and Kristjansson J. E.: The effects of domain choice on summer
642 precipitation simulation and sensitivity in a regional climate model, *J. Climate*, 11, 2698-2712,
643 1989.

644

645 Takahashi, H. G., & Polcher, J. (2019). Weakening of rainfall intensity on wet soils over the wet
646 Asian monsoon region using a high-resolution regional climate model. *Progress in Earth and*
647 *Planetary Science*, 6(1), 1-18.

648

649 Thorncroft, C. D. and Blackburn, M.: Maintenance of the African easterly jet, *Q. J. R. Meteorol*
650 *Soc.*, 125, 763–786, 1999.

651

652 Uppala S., Dee D., Kobayashi S., Berrisford P. and Simmons A.: Towards a climate data
653 assimilation system: status update of ERA-interim, *ECMWF Newsl.*, 15, 12–18, 2008.

654

655 Vinnikov K. Y. and Yeserkepova I. B.: Soil moisture: Empirical data and model results, *J. Clim.*,
656 4(1), 66–79, doi:10.1175/1520-0442(1991) 004<0066:SMEDAM>2.0.CO;2, 1991.

657

658 Vinnikov K. Y., Robock A., Speranskaya N. A. and Schlosser A.: Scales of temporal and spatial
659 variability of midlatitude soil moisture, *J. Geophys. Res.*, 101(D3), 7163–7174,
660 doi:10.1029/95JD02753, 1996.

661

662 Wang, G., Yu, M., Pal, J. S., Mei, R., Bonan, G. B., Levis, S., and Thornton, P. E.: On the
663 development of a coupled regional climate vegetation model RCM-CLM-CN-DV and its
664 validation its tropical Africa, *Clim. Dynam*, 46, 515–539, 2016.

665

666 Xue Y., De Sales F., Lau K. M. W., Bonne A., Feng J., Dirmeyer P., Guo Z., Kim K. M., Kitoh
667 A., Kumar V., Pocard-Leclercq I., Mahowald N., Moufouma-Okia W., Pegion P., Rowell D. P.,
668 Schemm J., Schulbert S., Sealy A., Thiaw W. M., Vintzileos A., Williams S. F. and Wu M. L.:
669 Intercomparison of West African Monsoon and its variability in the West African Monsoon
670 Modelling Evaluation Project (WAMME) first model Intercomparison experiment, *Clim.*
671 *Dynam.*, 35, 3–27, <https://doi.org/10.1007/s00382-010-0778-2>, 2010.

672

673 Zakey A. S., Solmon F., and Giorgi F.: Implementation and testing of a desert dust module in a
674 regional climate model, *Atmos. Chem. Phys.*, 6, 4687–4704, [https://doi.org/10.5194/acp-6-4687-](https://doi.org/10.5194/acp-6-4687-2006)
675 2006, 2006.

676

677 Zeng X., Zhao M. and Dickinson R. E.: Intercomparison of bulk aerodynamic algorithms for the
678 computation of sea surface fluxes using TOGA COARE and TAO DATA, *J. Climate*, 11, 2628-
679 2644, 1998.

680 Zhang, J., W.-C. Wang, and J. Wei, Assessing land-atmosphere coupling using soil moisture
681 from the Global Land Data Assimilation System and observational precipitation, *J. Geophys.*
682 *Res.*, 113, D17119, doi:10.1029/2008JD009807, 2008.

683 Zhang, J., W.-C. Wang, and L. R. Leung.: Contribution of land-atmosphere coupling to summer
684 climate variability over the contiguous United States, *J. Geophys. Res.*, 113, D22109,
685 doi:10.1029/2008JD010136, 2008.

686

687 Zhang, J. Y., L. Y. Wu, and W. Dong,: Land-atmosphere coupling and summer climate
688 variability over East Asia, *J. Geophys. Res.*, 116, D05117, doi 10.1029/2010JD014714, 2011.

689

690

691

692

693

694
695
696
697
698
699
700
701
702
703
704
705

Tables and figures:

	Central Sahel		West Sahel		Guinea		West Africa	
	PCC	MB (%)	PCC	MB (%)	PCC	MB (%)	PCC	MB (%)
CTRL_2003	0.98	-47.97	0.87	-75.76	0.82	-47.12	0.73	-49.31
CTRL_2004	0.98	-47.89	0.87	-68.35	0.85	-51.97	0.77	-50.56

706
707
708
709
710
711
712
713
714
715
716

Table1: The pattern correlation coefficient (PCC) and the mean bias (MB) for JJAS precipitation for model simulations with respect to CHIRPS, calculated for Guinea coast, central Sahel, west Sahel and the entire West African domain during the period 2003 and 2004.

717
718
719
720
721
722
723
724

		Central Sahel		West Sahel		Guinea coast		West Africa	
		Δ WC	Δ DC	Δ WC	Δ DC	Δ WC	Δ DC	Δ WC	Δ DC
Precipitation (%)	2003	13.80	-4.09	29.95	6.58	19.40	9.20	8.88	4.68
	2004	15.86	-3.29	38.58	-1.25	26.6	12.68	10.72	7.64
Temperature mean (°C)	2003	-1.48	0.56	-1.55	-0.41	-0.15	0.54	-0.62	0.50
	2004	-1.51	0.47	-1.15	-0.24	-0.19	0.59	-0.41	0.59
Sensible heat (w.m ⁻²)	2003	-16.89	8.57	-39.66	5.31	-2.41	7.52	-14.32	8.06
	2004	-19.53	7.55	-31.97	7.23	-3.01	9.18	-14.46	6.81
Latent heat (w.m ⁻²)	2003	21.27	-6.67	34.21	-6.06	3.09	-13.38	15.86	-8.07
	2004	28.55	-4.81	36.49	-6.20	7.09	-14.64	19.68	-8.53
PBL (m)	2003	-233.49	81.23	-293.23	-0.16	-94.42	132.74	-128.90	75.57
	2004	-223.06	49.48	-247.08	19.87	-119.38	146.80	-117.69	56.53

725

726 **Table2:** Table summarizing the maximum values of change obtained from the PDF distribution
 727 for precipitation, temperature, sensible heat, latent heat and PBL, calculated for Guinea coast,
 728 central Sahel, west Sahel and the entire West African domain during the period JJAS 2003 and
 729 JJAS 2004.

730

731

732

733

	Central Sahel		West Sahel		Guinea		West Africa	
	PCC	MB (°C)	PCC	MB (°C)	PCC	MB (°C)	PCC	MB (°C)
CTRL_2003	0.99	1.52	0.99	2.68	0.99	-0.34	0.99	0.85
CTRL_2004	0.99	1.50	0.99	2.14	0.99	-0.57	0.99	0.51

734

735 **Table3:** The pattern correlation coefficient (PCC) and the mean bias (MB) for JJAS 2m-
 736 temperature for model simulations with respect to CRU, calculated for Guinea coast, central
 737 Sahel, west Sahel and the entire West African domain during the period JJAS 2003 and JJAS
 738 2004.

739

740

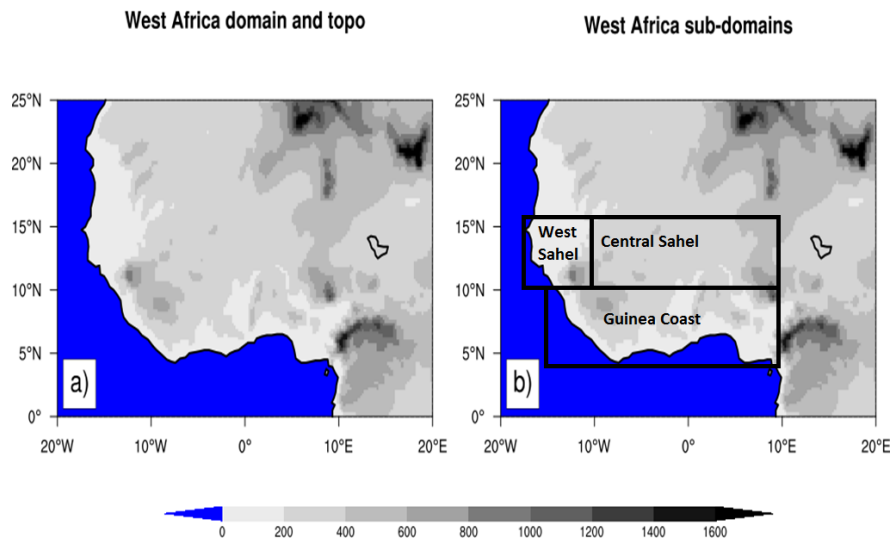
741

742

743

744

745



747

748 **Figure 1:** Topography of the West African domain. The analysis of the model result has an
749 emphasis on the whole West African domain and the three sub-regions Guinea coast, central
750 Sahel and west Sahel, which are marked with black boxes.

751

752

753

754

755

756

757

758

759

760

761

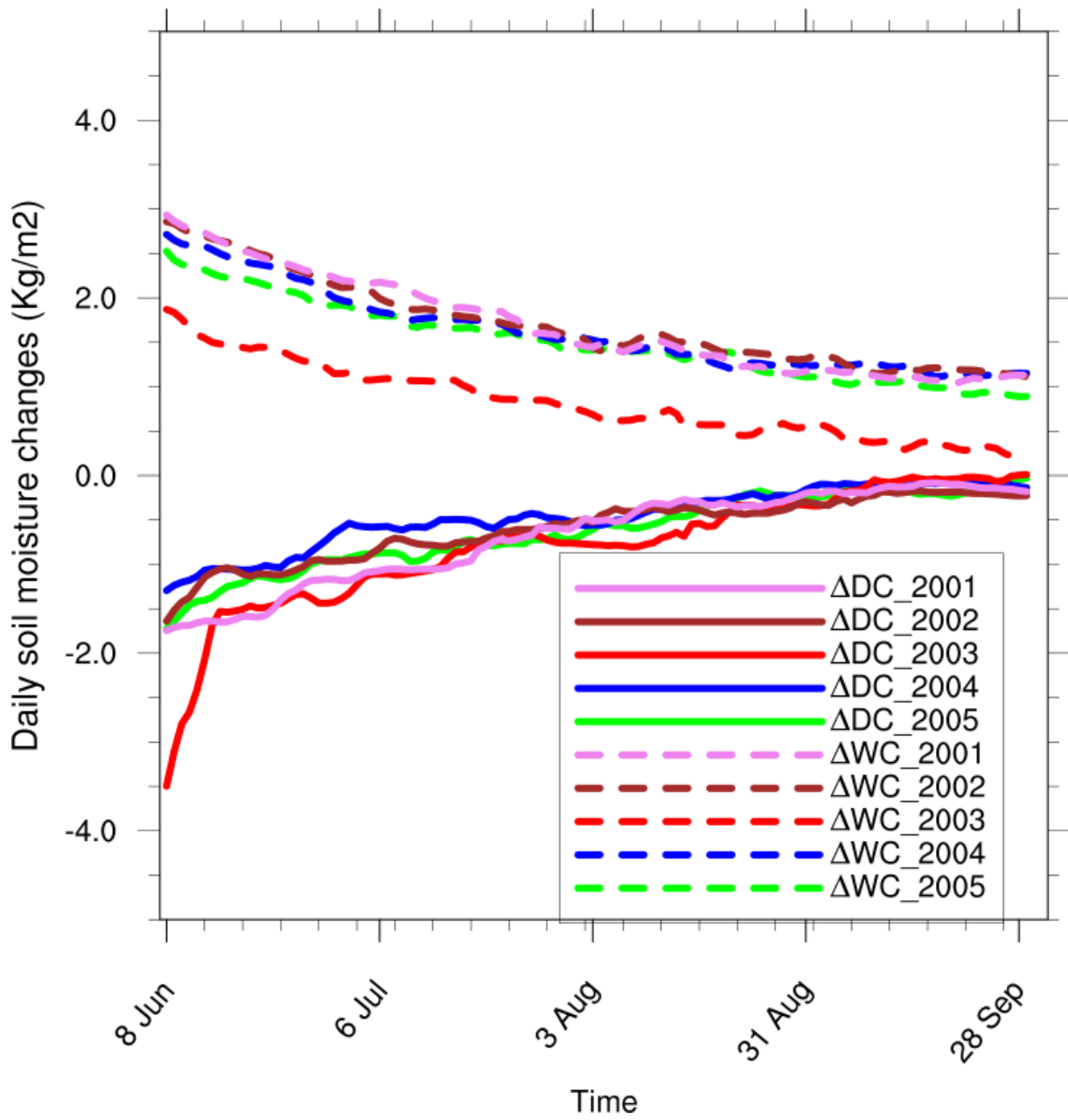
762

763

764

765
766
767
768
769
770
771

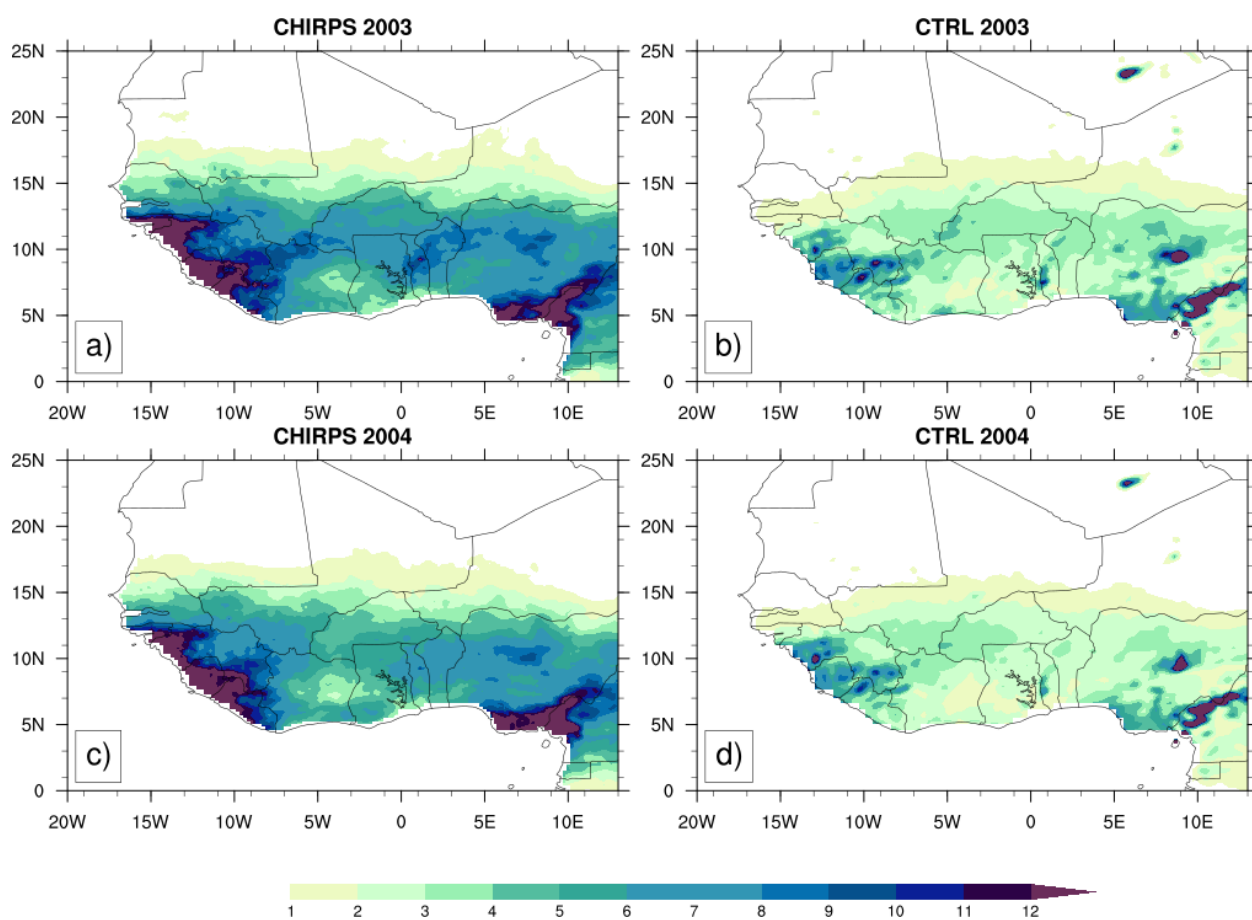
West Africa



772

773 **Figure 2:** Changes in daily soil moisture in the 5 runs (JJAS 2001 to 2005) over West African
774 domain, for the dry (ΔDC) and wet (ΔWC) experiments with respect to their corresponding
775 control experiment.

776
777
778
779
780

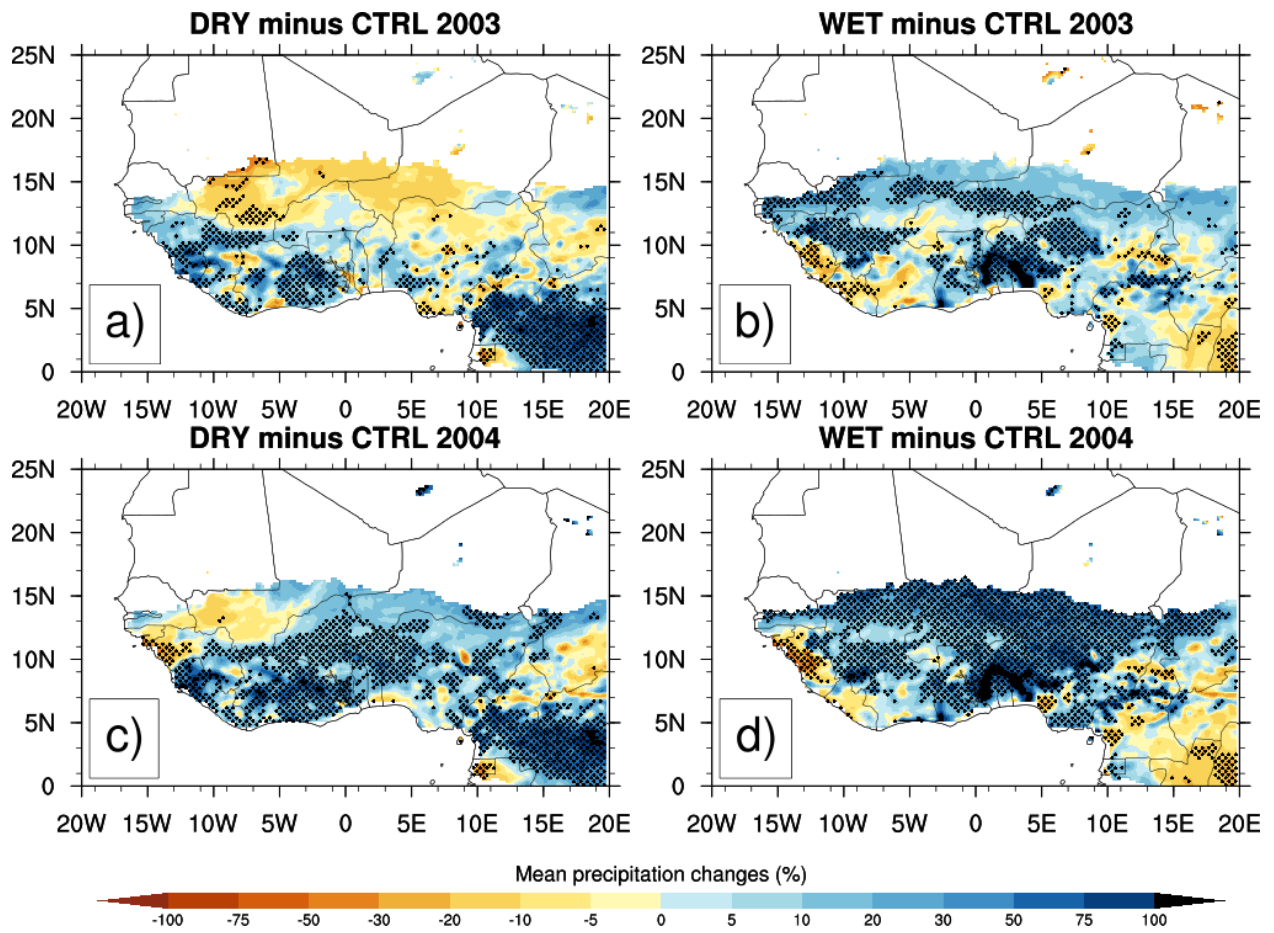


782

783 **Figure3:** Mean precipitation (mm/day) from CHIRPS (a, c) and the simulated control
784 experiments (CTRL) (b, d) with the reanalysis initial soil moisture ERA20C during JJAS 2003
785 and JJAS 2004.

786
787
788
789
790

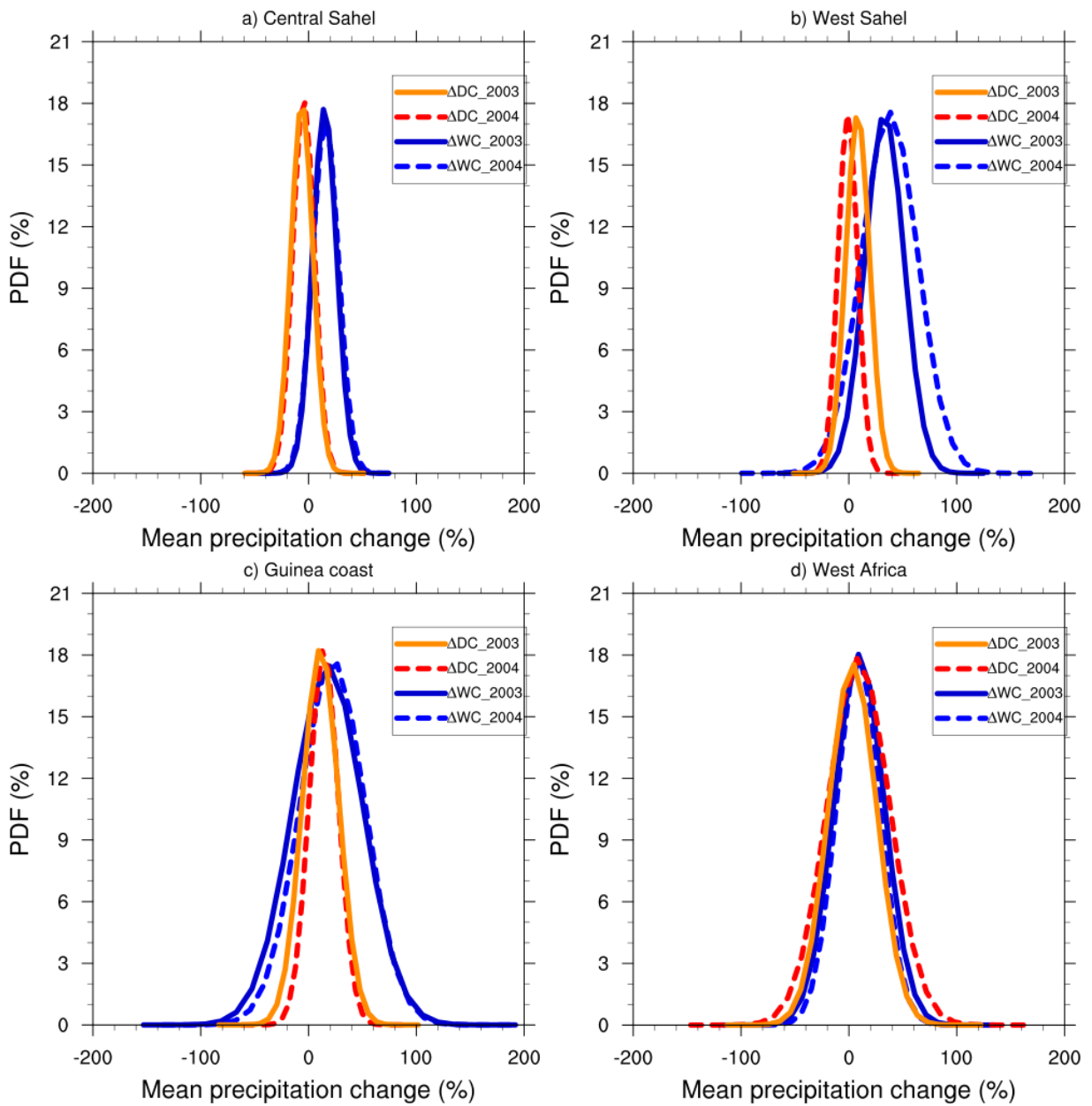
791
792
793
794
795
796
797
798



800
801 **Figure4:** Changes in mean precipitation (in %) for JJAS 2003 and JJAS 2004, from dry (resp. a
802 and c) and wet (resp. b and d) experiments with respect to the control experiment, the dotted area
803 shows differences that are statistically significant at 0.05 level.

804
805
806
807
808

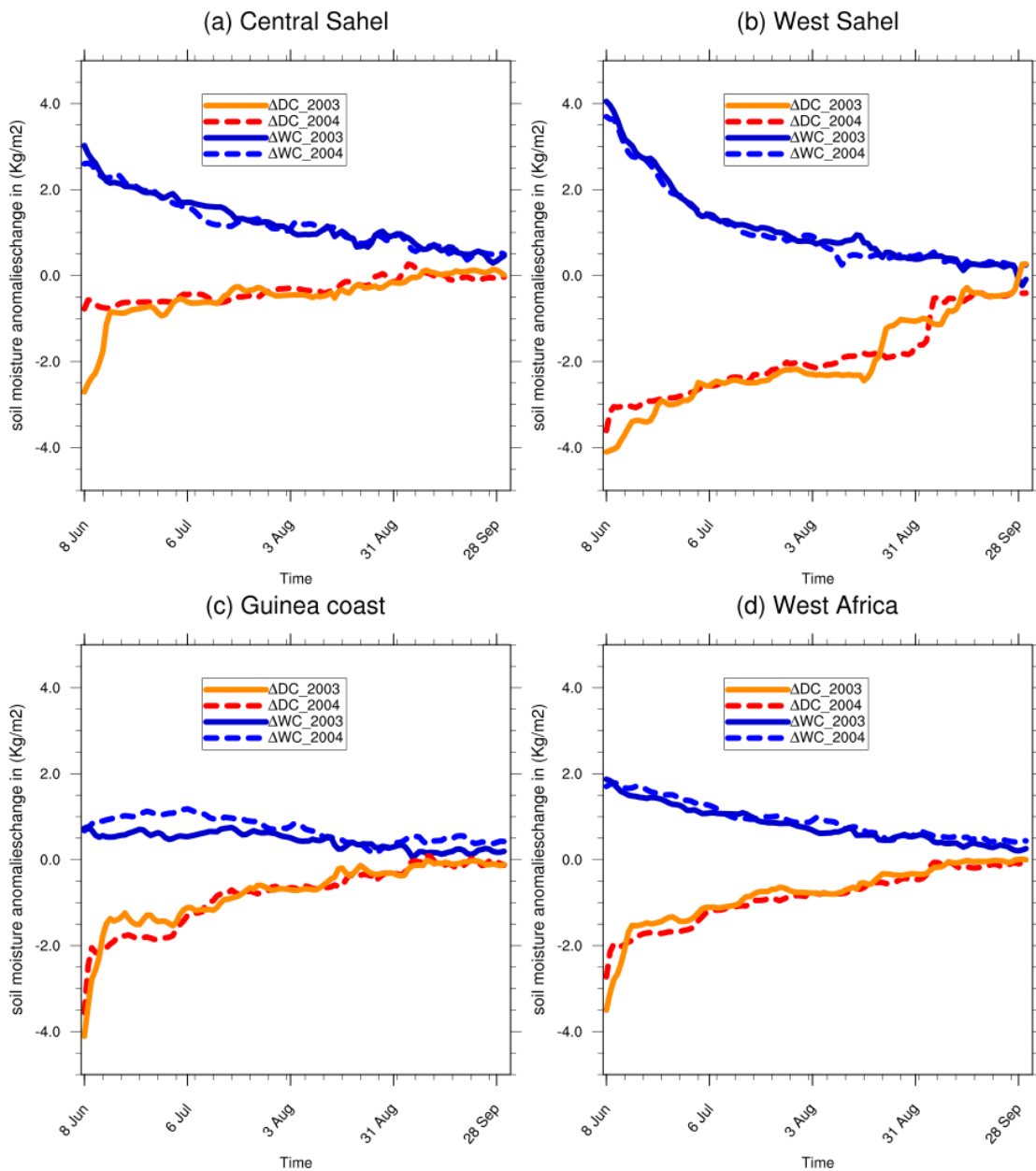
809
810
811
812
813
814
815
816
817



818

819 **Figure 5:** PDF distributions (%) of mean precipitation changes in JJAS 2003 and JJAS 2004,
 820 over (a) central Sahel, (b) West Sahel, (c) Guinea and (d) West Africa derived from dry (ΔDC)
 821 and wet (ΔWC) experiments compared to the control experiment.

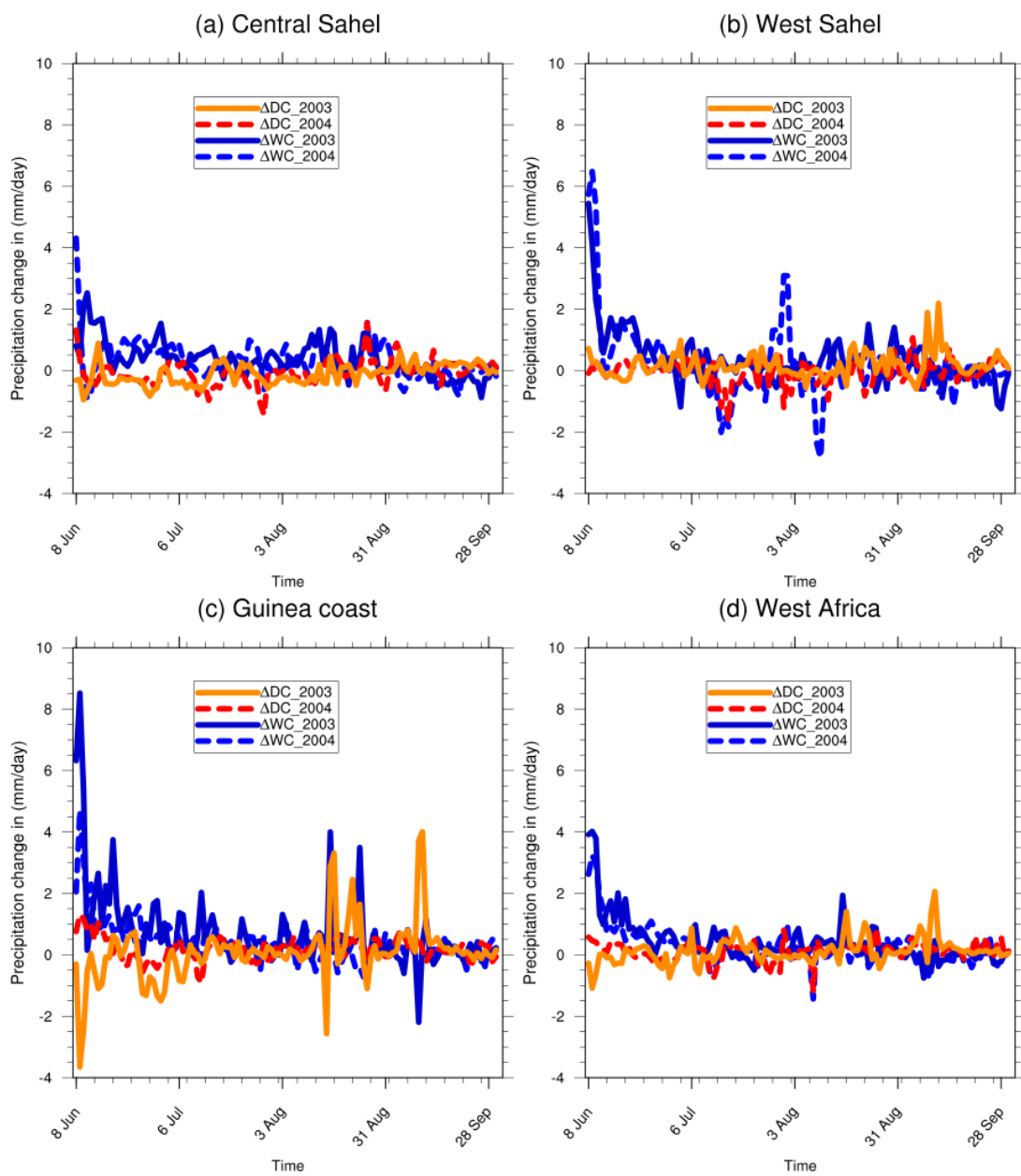
822
 823
 824
 825
 826
 827
 828
 829



830

831 **Figure 6:** Daily domain-average soil moisture changes for JJAS 2003 and JJAS 2004, from dry
832 (ΔDC) and wet (ΔWC) experiments with respect to the control experiment.

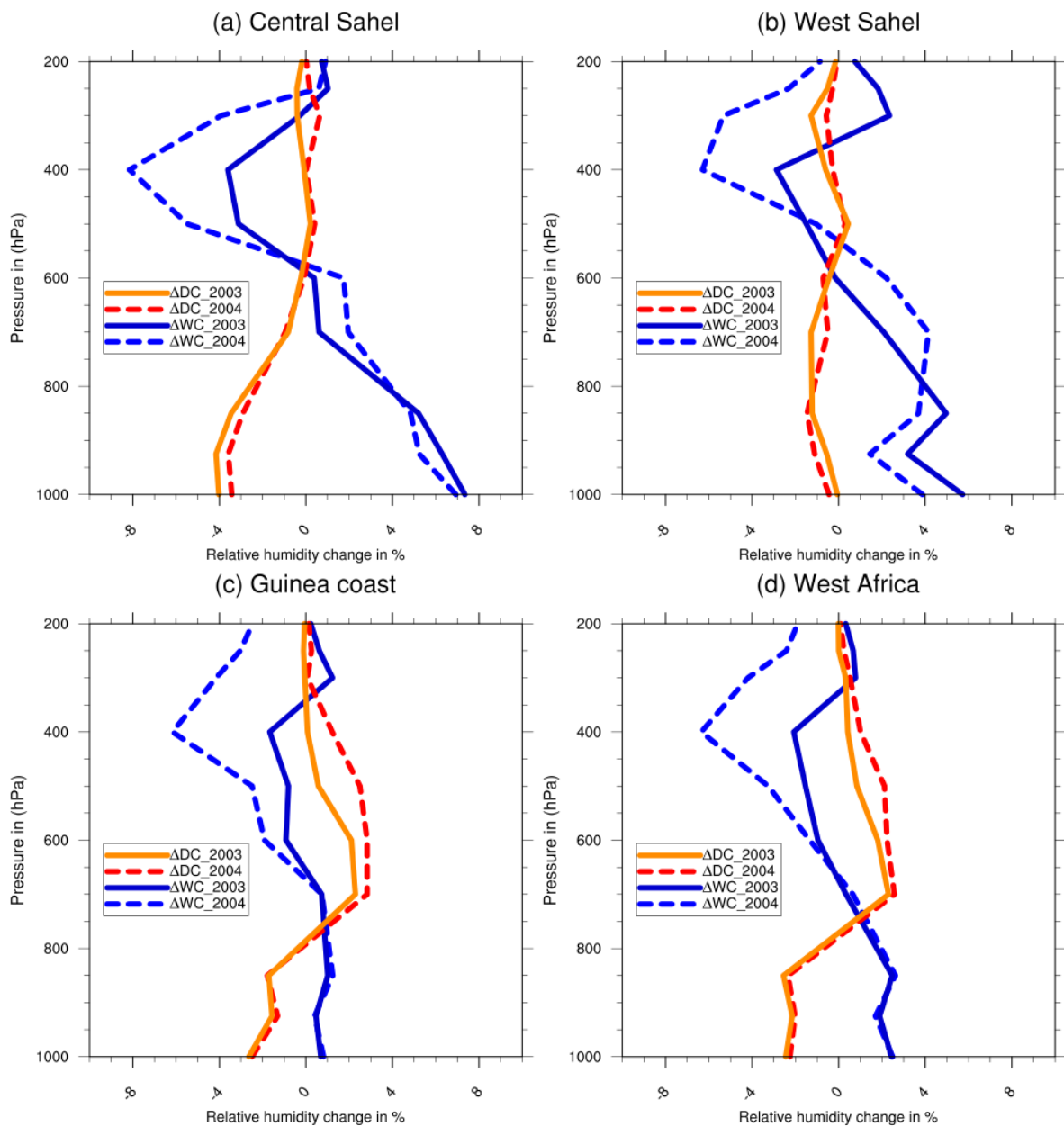
833
834
835
836
837
838
839
840



841
842

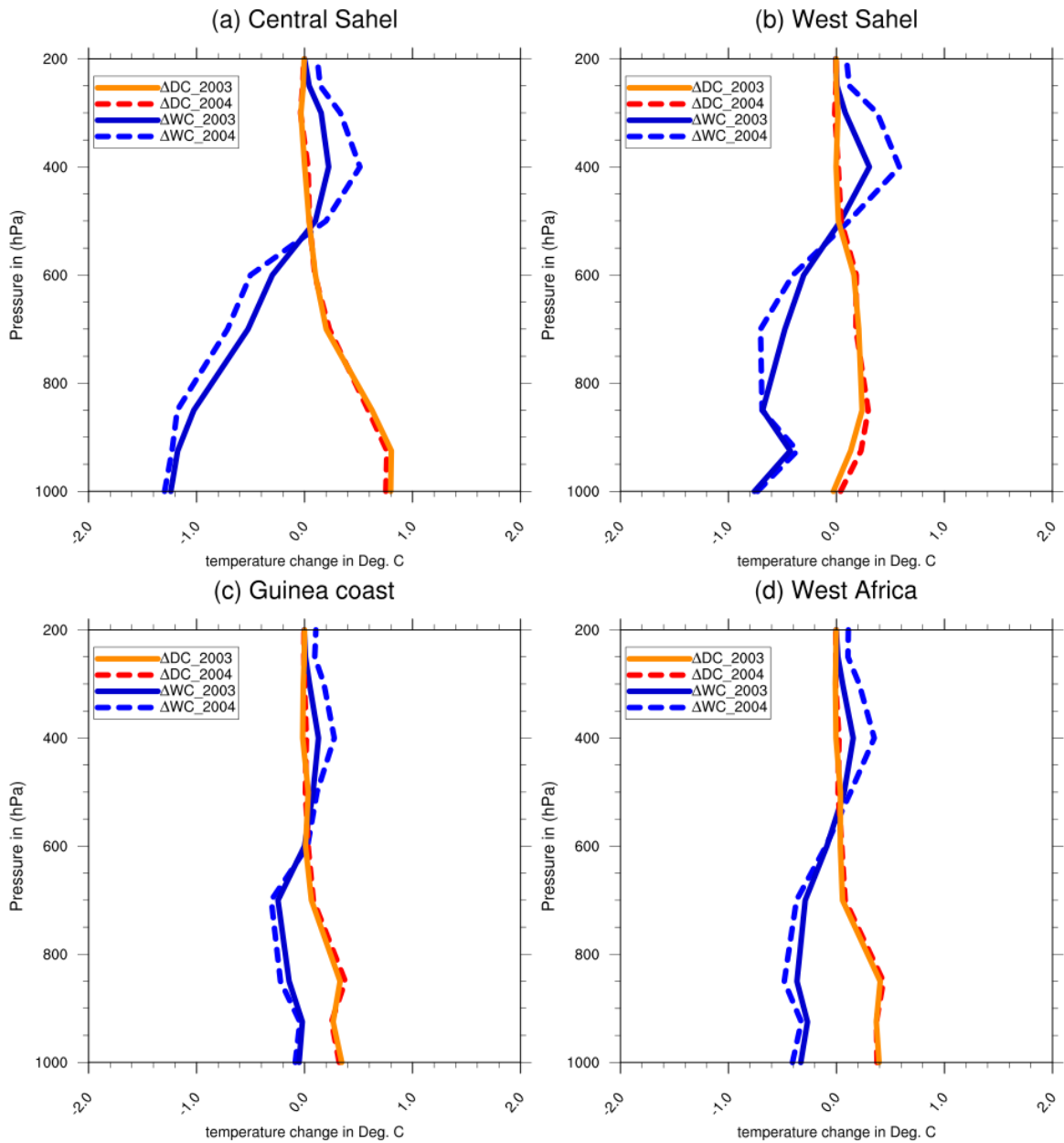
843
 844 **Figure 7:** Daily domain-average precipitation changes for JJAS 2003 and JJAS 2004, from dry
 845 (ΔDC) and wet (ΔWC) experiments with respect to the control experiment.

846
 847
 848
 849
 850
 851
 852

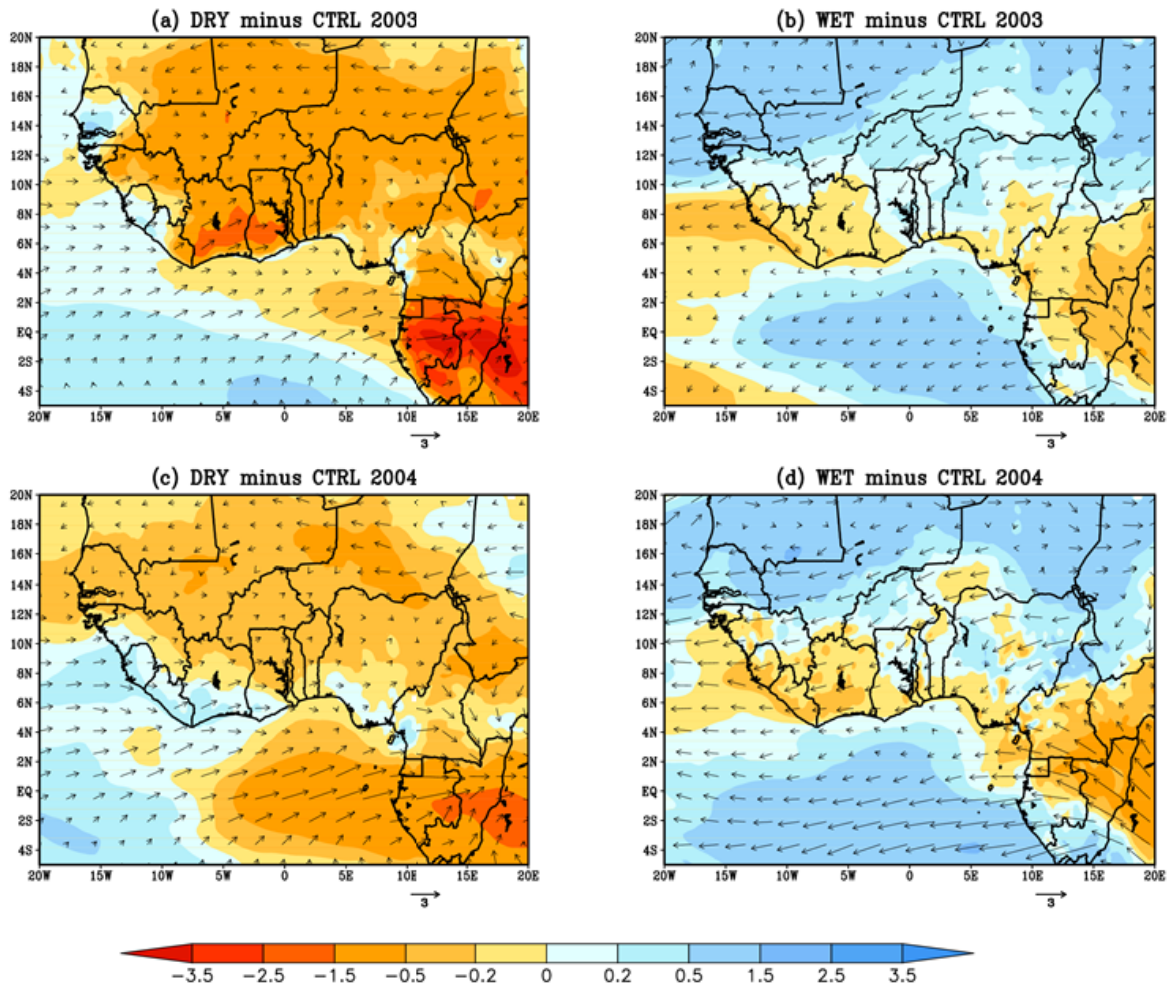


853
 854

855
 856 **Figure 8:** Vertical profile changes in Relative humidity for JJAS 2003 and JJAS 2004 from the
 857 dry (ΔDC) and wet (ΔWC) experiments with respect to corresponding control experiment over
 858 (a) central Sahel, (b) west Sahel, (c) Guinea coast, and (d) West Africa.
 859
 860

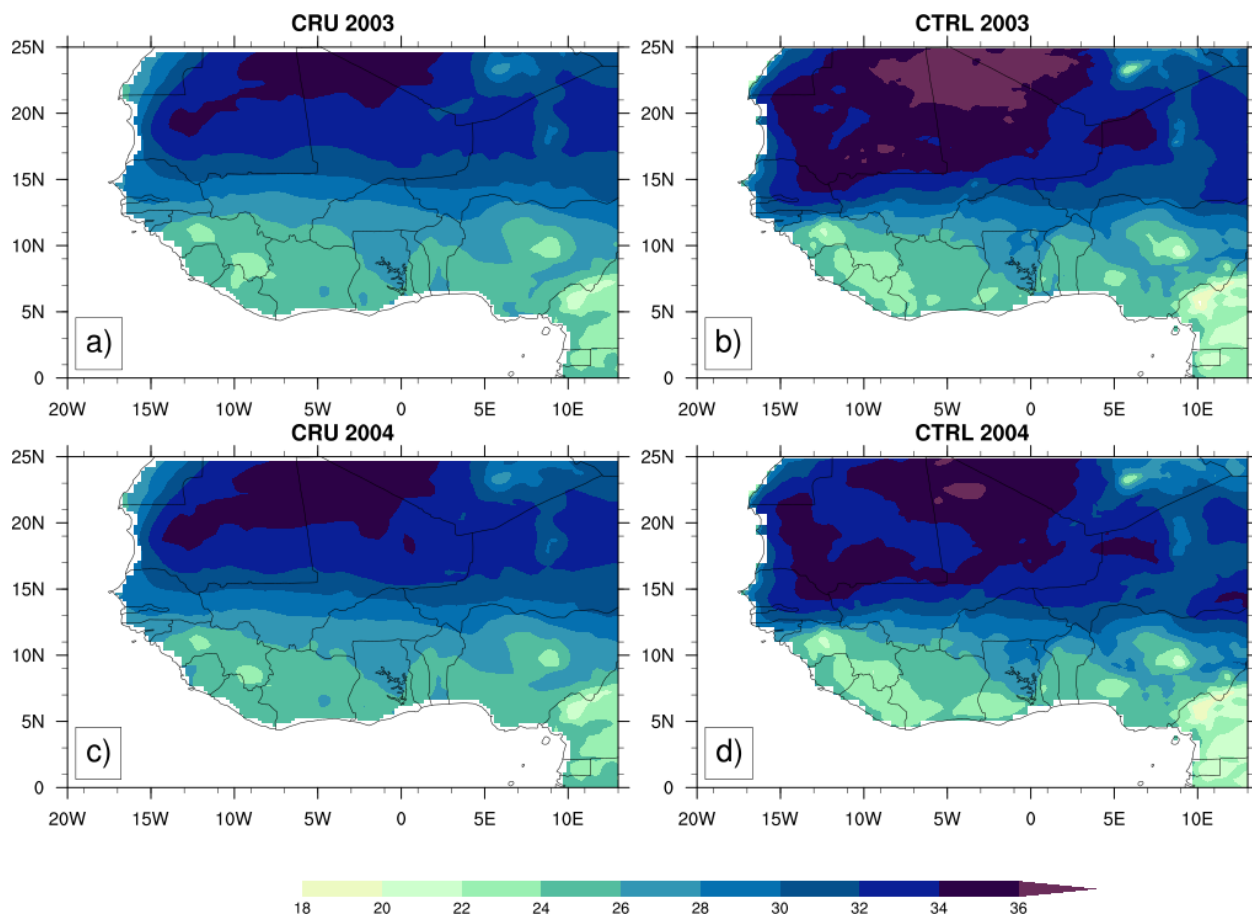


862 **Figure 9:** Vertical profile changes in temperature for JJAS 2003 and JJAS 2004 from the dry
 863 (ΔDC) and wet (ΔWC) experiments with respect to the control experiment over (a) central Sahel,
 864 (b) west Sahel, (c) Guinea coast, and (d) West Africa.
 865
 866



868 **Figure 10:** The lower tropospheric wind (850hpa) and moisture bias for JJAS 2003 and JJAS
 869 2004 from the dry (a and c) and wet (b and d) experiments with respect to the control
 870 experiment.

871
 872
 873
 874
 875
 876
 877
 878
 879
 880
 881
 882
 883



886

887 **Figure 11:** Mean 2m-temperature (°C) from CRU (a and c) for JJAS 2003 and JJAS 2004 and
888 the simulated control experiment (b and d) with the reanalysis initial soil moisture ERA20C.

889

890

891

892

893

894

895

896

897

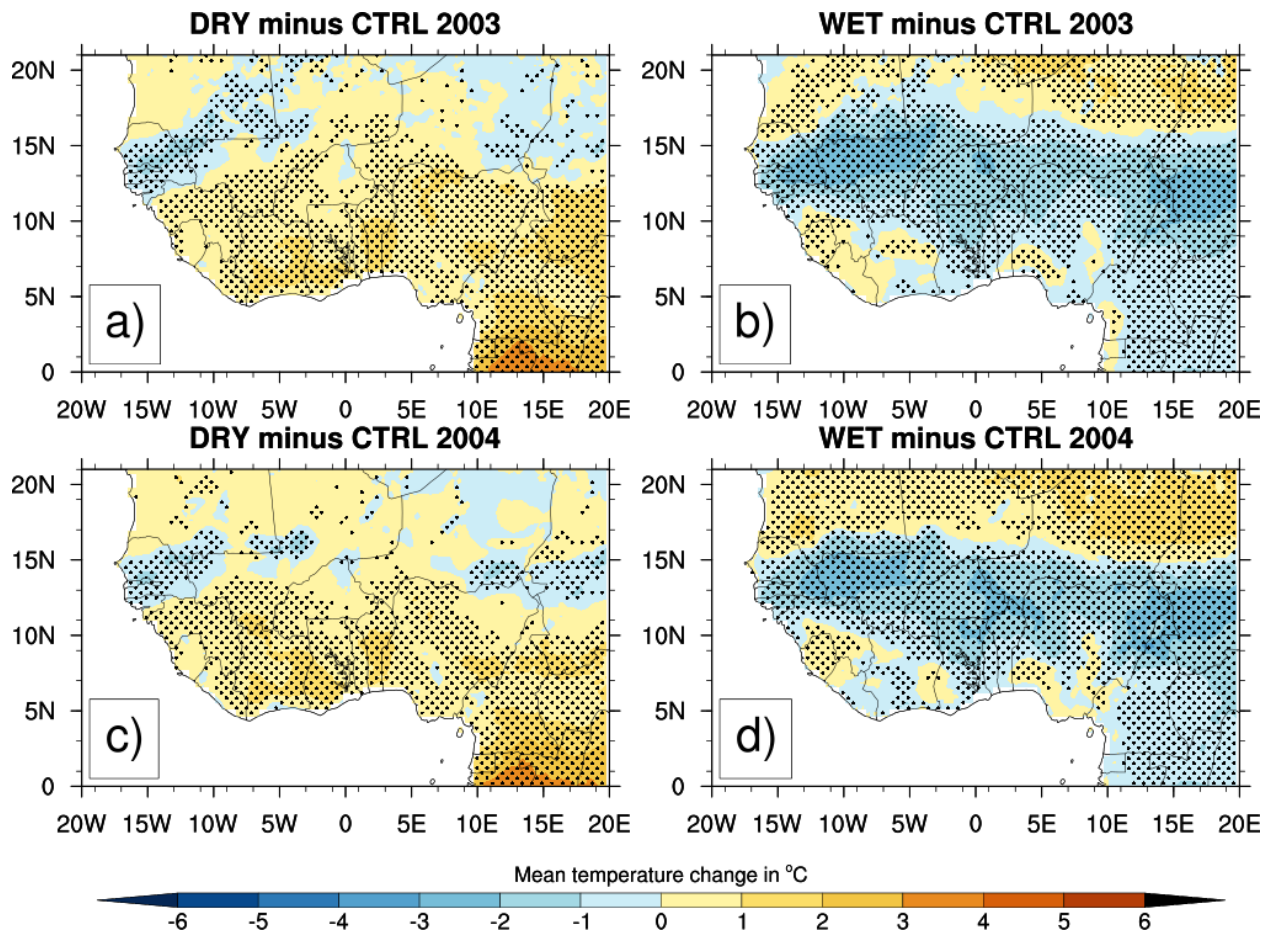
898

899

900

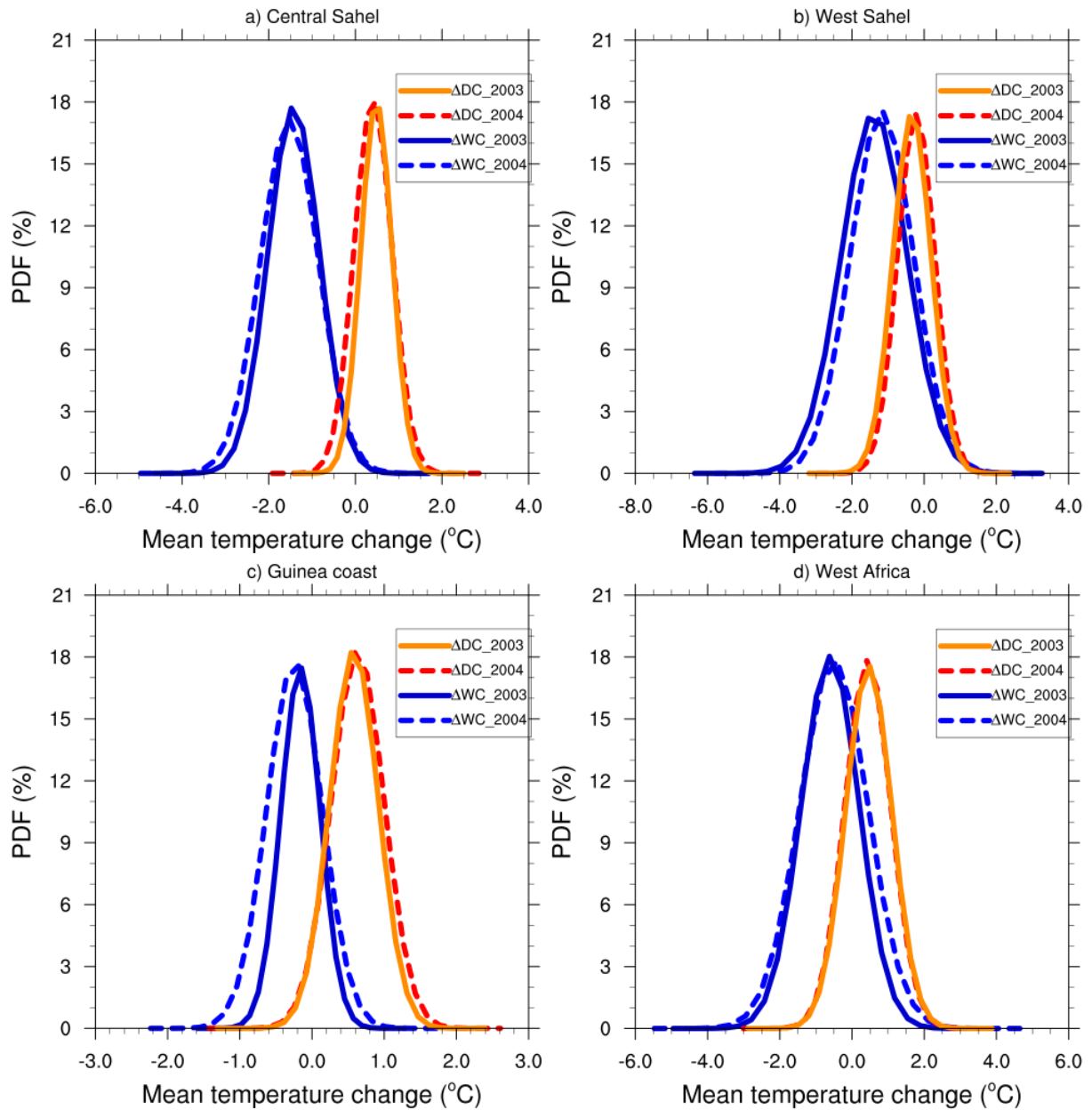
901

902
903



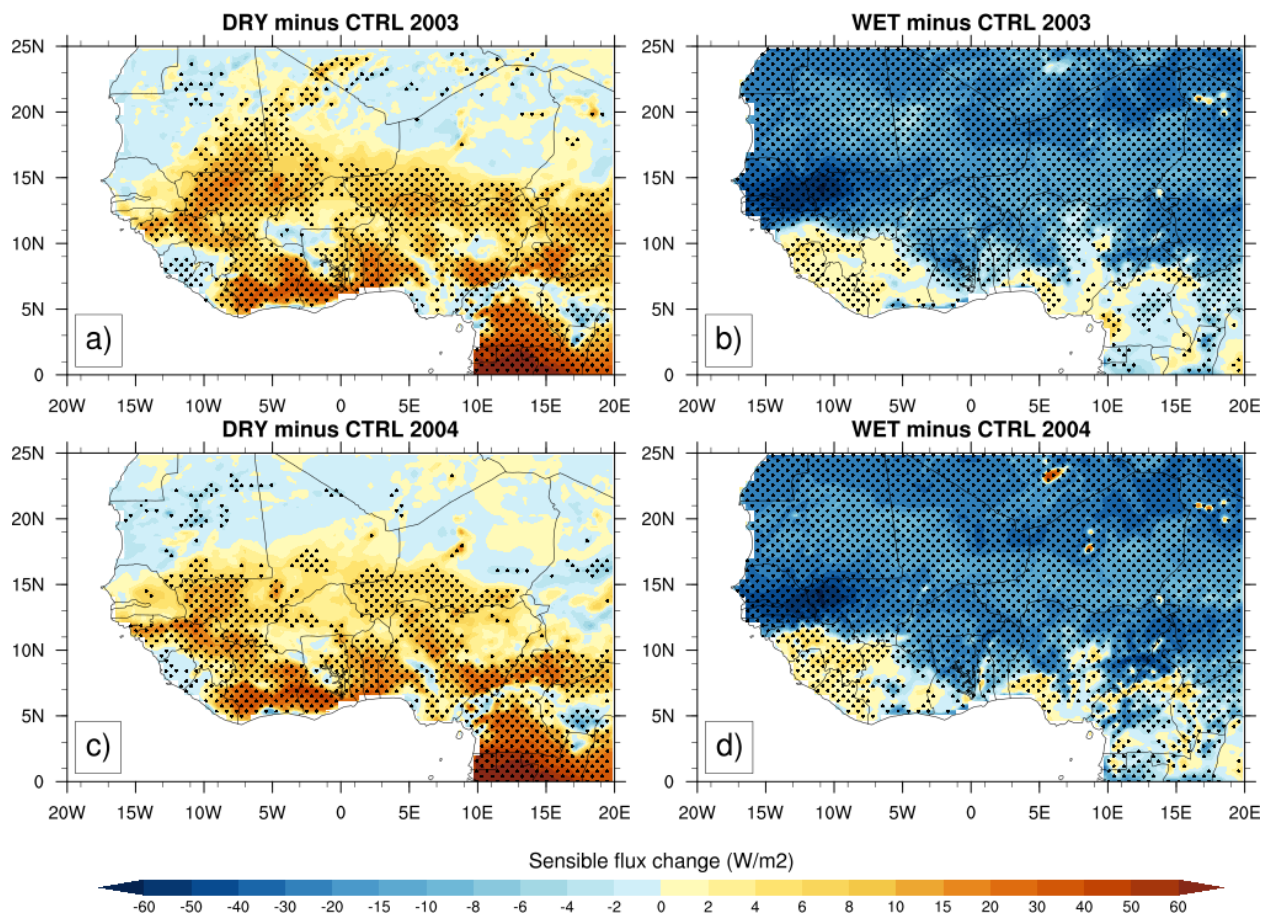
905
906 **Figure 12:** Changes in 2m-temperature (°C) for JJAS 2003 and JJAS 2004, from dry (resp. a and
907 c) and wet (resp. b and d) experiments with respect to the control experiment, the dotted area
908 shows differences that are statistically significant at 0.05 level.

909
910
911
912
913
914
915
916
917
918
919



921
 922 **Figure 13:** PDF distributions (%) of mean temperature changes in JJAS 2003 and JJAS 2004,
 923 over (a) central Sahel, (b) West Sahel, (c) Guinea and (d) West Africa derived from dry (ΔDC)
 924 and wet (ΔWC) experiments compared to the control experiment.

925
 926
 927
 928
 929
 930



932

933 **Figure 14:** Same as Fig.12 but for sensible heat fluxes (in $W.m^{-2}$).

934

935

936

937

938

939

940

941

942

943

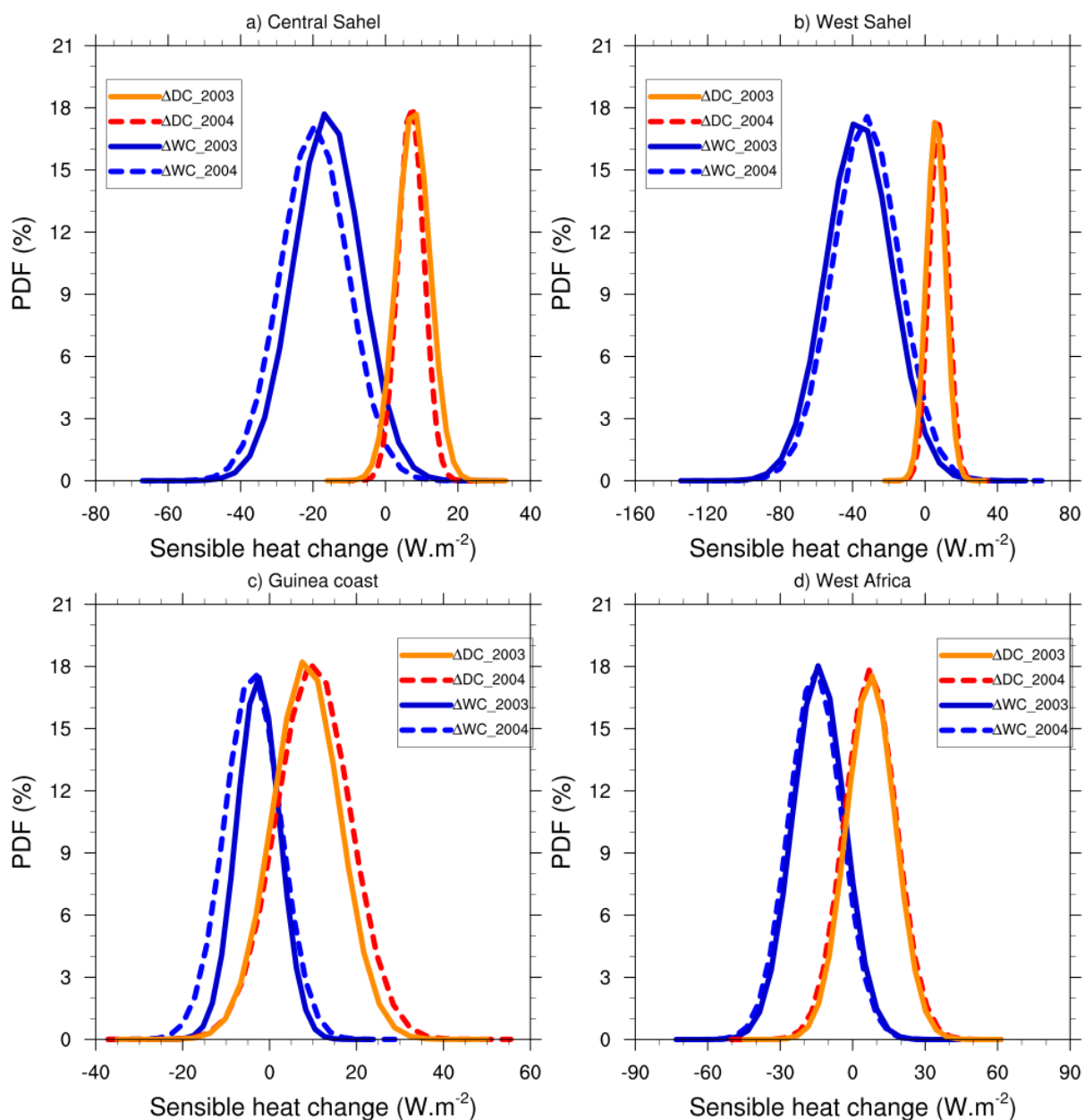
944

945

946

947

948



951

952 **Figure 15:** Same as Fig.13 but for sensible heat fluxes (in $W.m^{-2}$).

953

954

955

956

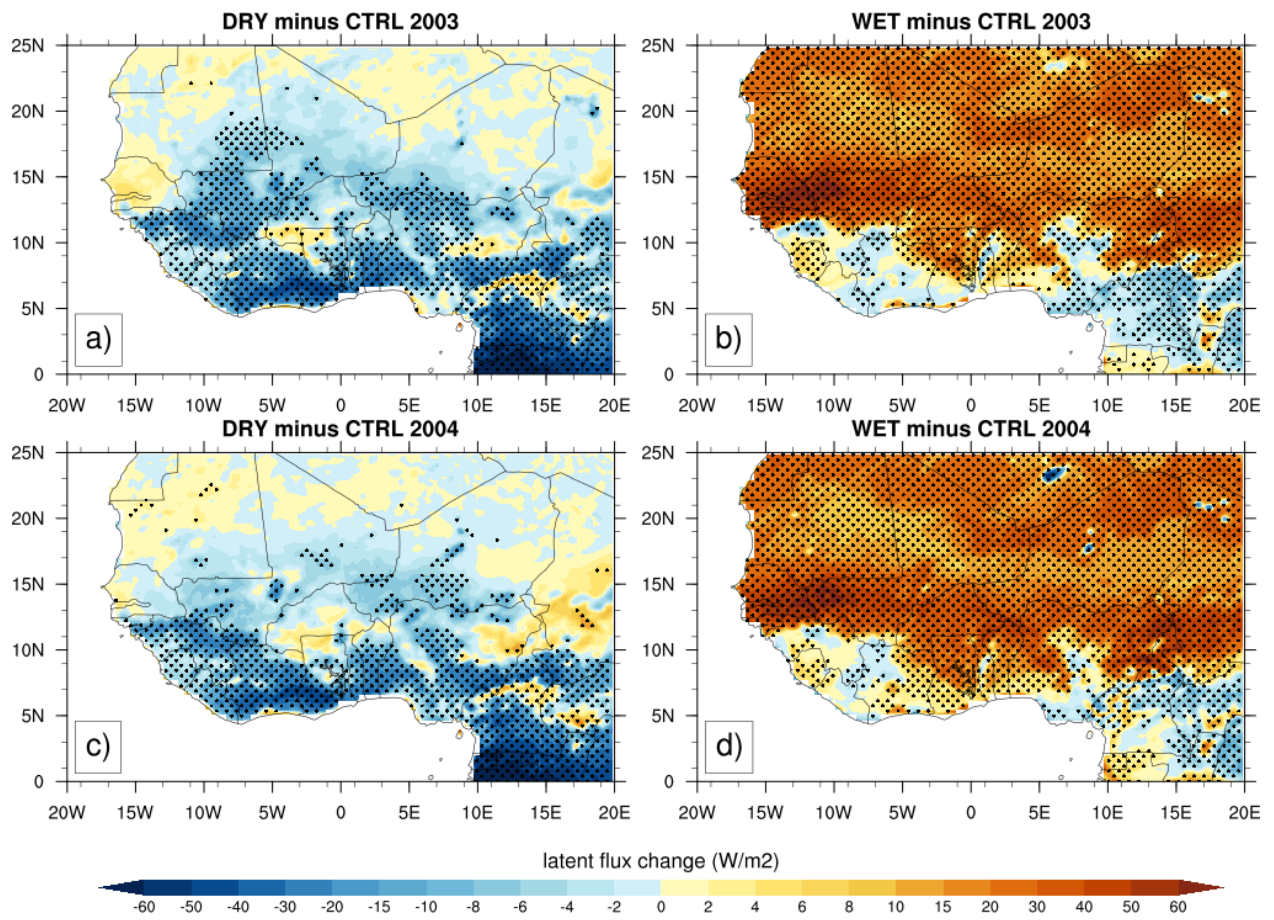
957

958

959

960

961



963

964 **Figure 16:** Same as Fig.12 but for latent heat fluxes (in $W.m^{-2}$).

965

966

967

968

969

970

971

972

973

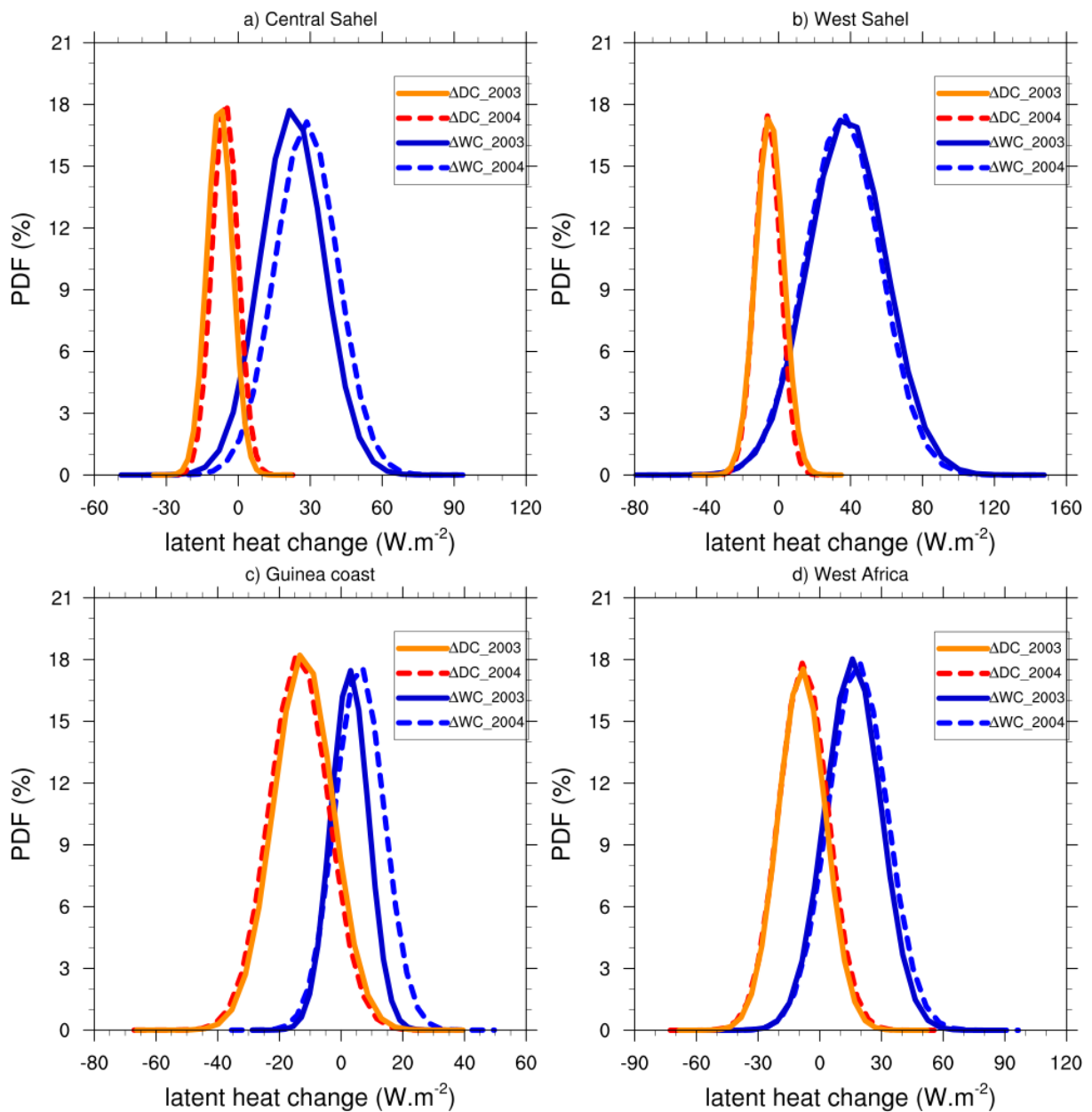
974

975

976

977

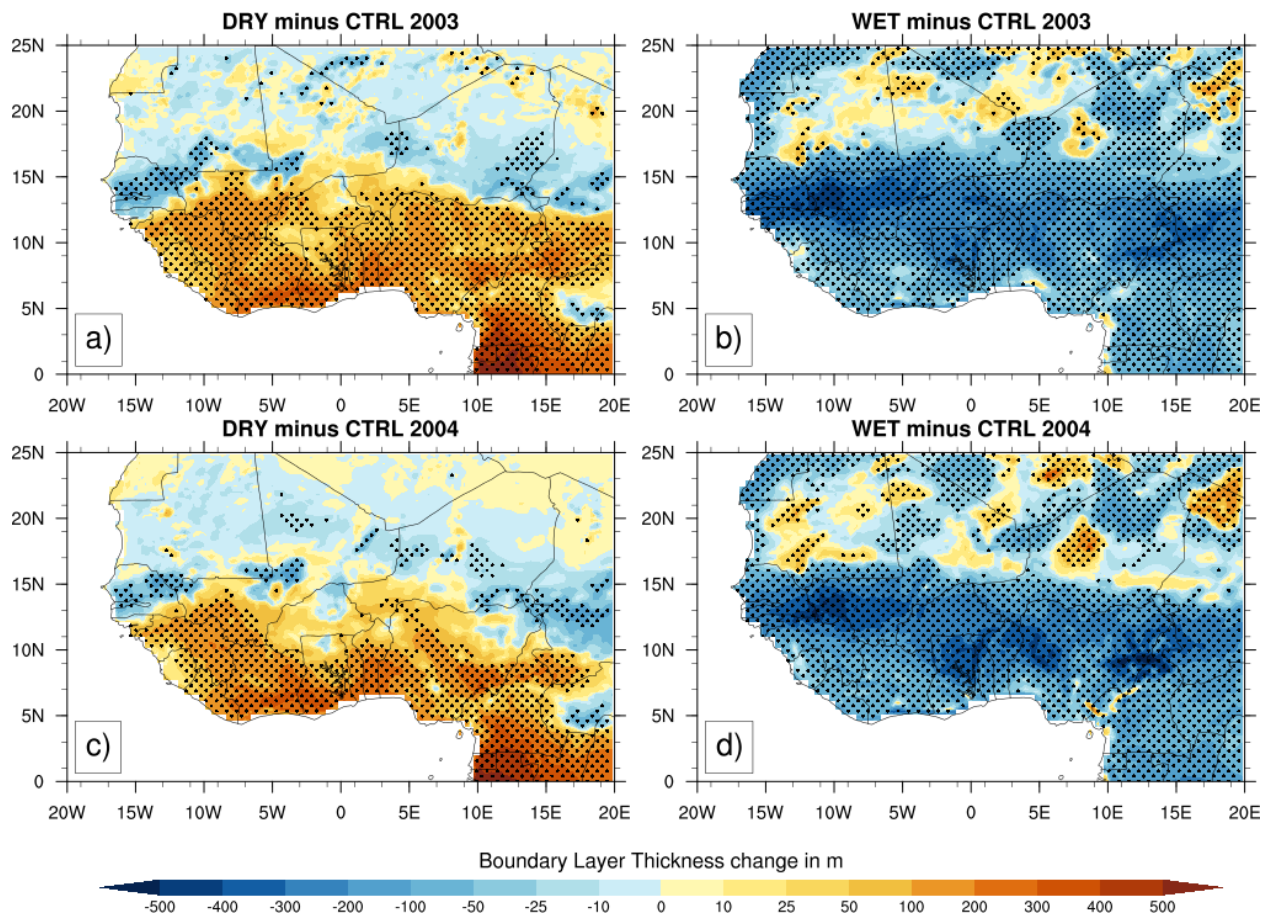
978



980
 981
 982
 983
 984
 985
 986
 987
 988
 989
 990

Figure 17: Same as Fig.13 but for latent heat fluxes (in $W.m^{-2}$).

991



993

994 **Figure 18:** Same as Fig.12 but for the change of the height of the planetary boundary layer (in
995 m).

996

997

998

999

1000

1001

1002

1003

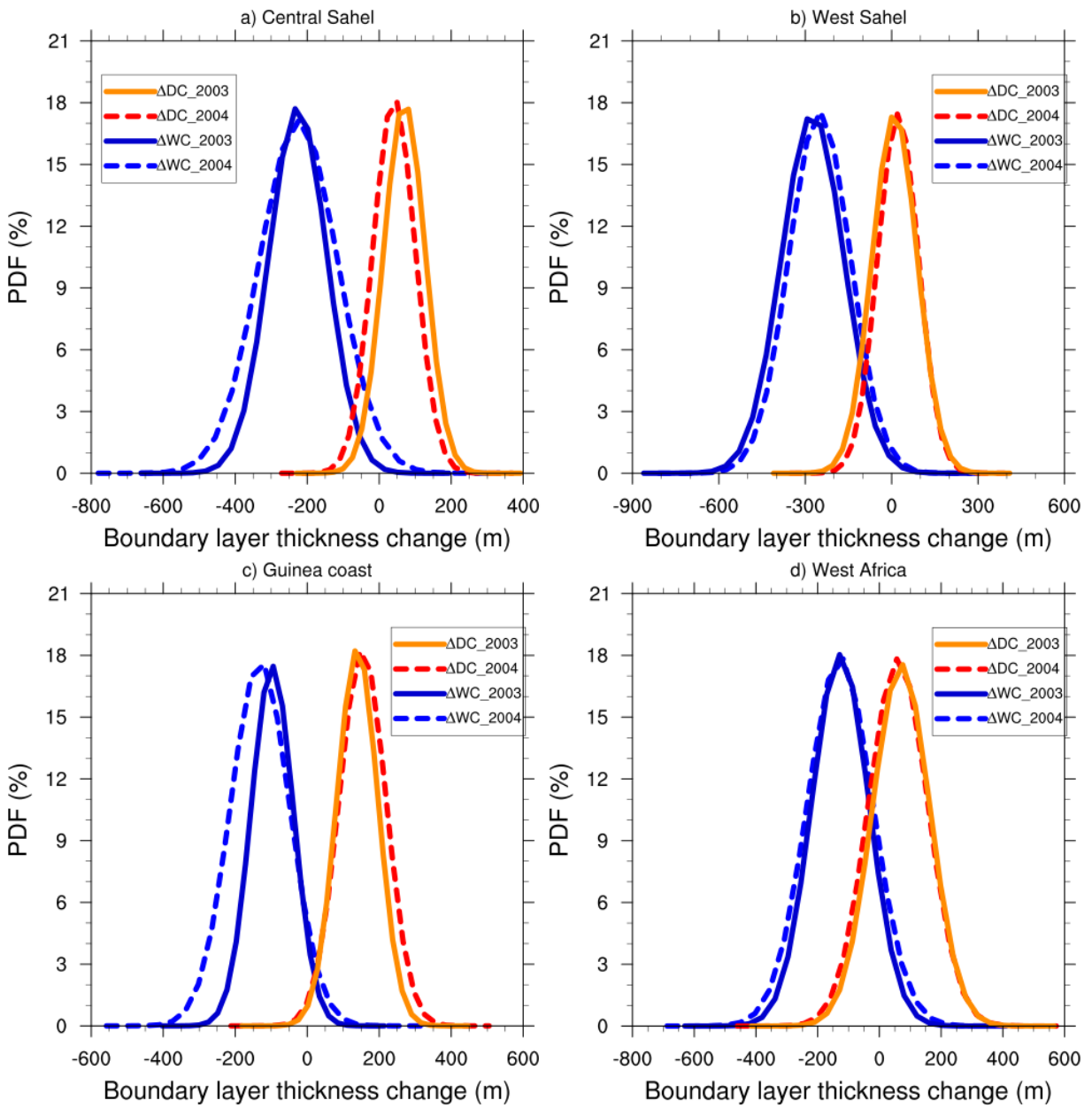
1004

1005

1006

1007

1008



1011

1012 **Figure 19:** Same as Fig.13 but for the height of the planetary boundary layer (in m).

1013

1014

1015

1016

1017

1018

1019